nature ecology & evolution

ARTICLES

https://doi.org/10.1038/s41559-022-01808-w

A single gene integrates sex and hormone regulators into sexual attractiveness

Nan Chen[1,2,3,4,9], Yong-Jun Liu[1,9], Yong-Liang Fan[2]✉, Xiao-Jin Pei[1,2], Yang Yang[1], Ming-Tao Liao[1], Jiru Zhong[1], Na Li[1,4], Tong-Xian Liu[2,5], Guirong Wang[6], Yufeng Pan[7], Coby Schal[8] and Sheng Li[1,3,4]✉

Sex differentiation and hormones are essential for the development of sexual signals in animals, and the regulation of sexual signals involves complex gene networks. However, it is unknown whether a core gene is able to connect the upstream regulators for controlling sexual signal outputs and behavioural consequences. Here, we identify a single gene that integrates both sex differentiation and hormone signalling with sexual attractiveness in an insect model. *CYP4PC1* in the German cockroach, *Blattella germanica*, controls the rate-limiting step in producing female-specific contact sex pheromone (CSP) that stimulates male courtship. As revealed by behavioural, biochemical, molecular, genetic and bioinformatic approaches, in sexually mature females, *CYP4PC1* expression and CSP production are coordinately induced by sex differentiation genes and juvenile hormone (JH) signalling. In adult males, direct inhibition of *CYP4PC1* expression by doublesex^{M} binding in gene promoter and lack of the gonadotropic hormone JH prevent CSP production, thus avoiding male–male attraction. By manipulating the upstream regulators, we show that wild-type males prefer to court cockroaches with higher *CYP4PC1* expression and CSP production in a dose-dependent manner, regardless of their sex. These findings shed light on how sex-specific and high sexual attractiveness is conferred in insects.

'By riverside are cooing, a pair of turtledoves; a good young male is wooing, a pretty female he prefers'. As implied by a saying in the Book of Songs (an ancient Chinese poetry classic), sexual signals evoke sexual attraction. As a key driver of sexual selection, sexual attraction involves both emission and reception of sexual signals[1,2]. Most animals have evolved species-specific sexual signals, such as tail colour and length, song quality and amplitude, and unique pheromone blends, that are highly attractive to potential sexual partners[1]. Sensed through vision, audition, olfaction, taste and touch, and interpreted in brain networks, sexual signals elicit sexual interest, courtship and ultimately copulation. Chemical communication stimuli are pivotal sexual signals in mammals, and their production is regulated by sex steroid hormones[2]. Moreover, sex differentiation directs somatic cell specification, leading to the development of distinct sex glands, ovaries and testes, and thus the production of sex-specific steroid hormones[3,4]. Nevertheless, it is poorly understood how sex differentiation and sex-specific hormones are integrated for controlling the production of sexual signals.

Sex-specific sexual signals have been investigated in many insects. In the fruit fly, *Drosophila melanogaster*, sex differentiation affects sexual signals and attraction, as do insect hormones[5,6]. Many insects rely on volatile sex pheromones for mate-finding, and non-volatile contact sex pheromones (CSPs) in the final species- and sex-recognition and mate choice[7]. The German cockroach, *Blattella germanica*, is a well-studied species regarding sex pheromone chemistry and sexual behaviours, and thus serves as an excellent insect model for studying reciprocal sexual signalling between the sexes[7,8]. Sexually receptive female cockroaches produce a volatile sex pheromone, blattellaquinone, that guides males to the female[9], and a blend of hydrocarbon-derived CSP components that elicit close-range male courtship, which also enables females to assess males and engage in mate choice[8,10,11]. The CSP consists of two homologous series of C_{27} and C_{29} methyl ketones, alcohols and aldehydes, and each component can independently elicit courtship[8]. The most abundant CSP component is 3,11-dimethylnonacosan-2-one (C_{29} methyl ketone)[8,12], which is derived through hydroxylation and subsequent oxidation of its 3,11-dimethylnonacosane precursor at the 2-position[13]. Being female- and age-specific and induced by the insect gonadotropic hormone, juvenile hormone (JH), the hydroxylation step, mediated by a putative cytochrome P450 (*CYP*) gene, was shown to be a rate-limiting step in CSP production[13] (Extended Data Fig. 1). However, the identity of this putative *CYP* gene and the molecular mechanism behind how it connects and integrates upstream regulatory elements with sexual attractiveness have remained unknown for 30 years.

Here, using behavioural, biochemical, molecular, genetic and bioinformatic approaches, we identify a single gene, *CYP4PC1*, that controls CSP production and sexual attractiveness by acting as a core integrator of sex differentiation and hormone pathways. This discovery reveals how high sexual attractiveness is achieved on maturation and, most importantly, only in females, making them sexually attractive to wild-type (WT) males. Moreover, by manipulating the

[1]Guangdong Provincial Key Laboratory of Insect Developmental Biology and Applied Technology, Institute of Insect Science and Technology, School of Life Sciences, South China Normal University, Guangzhou, China. [2]State Key Laboratory of Crop Stress Biology for Arid Areas, and Key Laboratory of Integrated Pest Management on the Loess Plateau of Ministry of Agriculture, Northwest A&F University, Yangling, China. [3]Guangdong Laboratory for Lingnan Modern Agriculture, Guangzhou, China. [4]Guangmeiyuan R&D Center, Guangdong Provincial Key Laboratory of Insect Developmental Biology and Applied Technology, South China Normal University, Meizhou, China. [5]Laboratory of Insect Ecology and Molecular Biology, College of Plant Health and Medicine, Qingdao Agricultural University, Qingdao, China. [6]Lingnan Guangdong Laboratory of Modern Agriculture, Genome Analysis Laboratory of the Ministry of Agriculture, Agricultural Genomics Institute at Shenzhen, Chinese Academy of Agricultural Sciences, Shenzhen, China. [7]The Key Laboratory of Developmental Genes and Human Disease, School of Life Science and Technology, Southeast University, Nanjing, China. [8]Department of Entomology and Plant Pathology, North Carolina State University, Raleigh, NC, USA. [9]These authors contributed equally: Nan Chen, Yong-Jun Liu. ✉e-mail: yfan@nwsuaf.edu.cn; lisheng@scnu.edu.cn

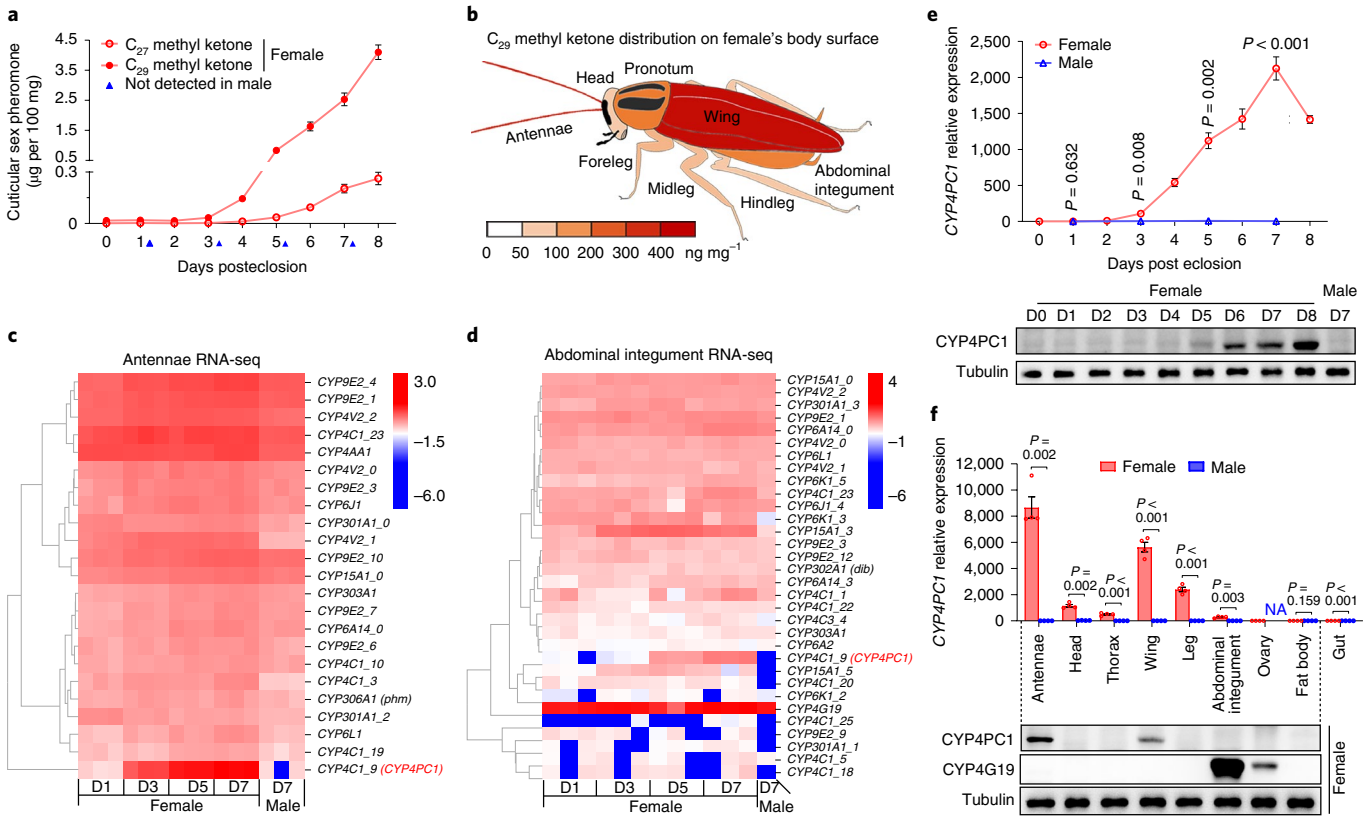

Fig. 1 | Screening of *CYP* candidates for CSP biosynthesis. a, Cuticular C_{27} and C_{29} methyl ketone accumulation in virgin females during the first vitellogenic cycle. $n = 6$ biological replicates. **b**, A colour diagram of C_{29} methyl ketone distribution on the body surface of a sexually mature female. Detailed statistical analyses are shown in Extended Data Fig. 2a. **c**,**d**, Heatmap representation (log_{10} fold change) of 23 upregulated *CYP*s in the antennae (**c**), and 32 upregulated *CYP*s in the abdominal integument (**d**) of females compared to males, and their transcriptional dynamics during sexual maturation. FPKM values underlying the heatmaps are available in Supplementary Tables 1 and 2. **e**, Temporal changes of *CYP4PC1* mRNA and protein levels from the antennae during the first vitellogenic cycle. $n = 4$ biological replicates. **f**, Tissue distribution of *CYP4PC1* mRNA and protein in sexually mature females (day 7). $n = 4$ biological replicates. NA, not applicable in males. *P* values were determined by two-tailed unpaired *t*-test (**e**,**f**). Males used as a control in **a**–**f**. Data in **a**,**e**,**f** are mean ± s.e.m.

upstream regulators of *CYP4PC1*, we show that feminized adult males could be more attractive to WT males than sexually mature females.

Results

Screening of *CYP* candidates for CSP production. As a first step towards screening of key genes involved in the cockroach CSP biosynthetic pathway, we investigated changes in two cuticular CSP components, C_{29} and C_{27} methyl ketones, across tissues and ages in both sexes. The two methyl ketones were not detected in adult males, but they consistently increased in females during the first vitellogenic cycle (Fig. 1a). The most abundant C_{29} methyl ketone was distributed throughout the female's body surface, and was present in considerably higher concentration on the antennae and wings than in other body parts (Fig. 1b and Extended Data Fig. 2a), suggesting that the antennae and wings may serve as the major sites of CSP production or accumulation.

To screen for the putative sex- and age-specific *CYP* gene that encodes the rate-limiting hydroxylase[13], we performed comparative RNA-sequencing (RNA-seq) analysis of female antennae at different ages, using male antennae as a negative control. Compared to the males, 23 *CYP* genes showed a significant upregulation in sexually mature (day 7) females, of which *C0J52_06753* (previously named *CYP4C1_9* by genomic annotation)[14] exhibited the highest expression (Extended Data Fig. 2b, left and Supplementary Table 1). Moreover, its expression in the female antennae consistently increased during the first vitellogenic cycle (Fig. 1c), resembling the developmental pattern of cuticular CSP production. Similar results were obtained from RNA-seq of abdominal integument (Fig. 1d, Extended Data Fig. 2b, right and Supplementary Table 2), which was previously proposed as the major site of CSP biosynthesis[15]. Nevertheless, this gene showed much higher relative expression in the antennae than in the abdominal integument (Supplementary Tables 1 and 2). The full length of *C0J52_06753* encodes 507 amino acid residues containing conserved P450 motifs (Extended Data Fig. 2c), and was assigned to a new 4PC subfamily and named *CYP4PC1* (GenBank no. MZ962381) by the P450 nomenclature committee. Real-time quantitative PCR (qPCR) and western blotting were then performed to validate the spatio-temporal pattern of *CYP4PC1* expression. The same as CSP production, both *CYP4PC1* messenger RNA and protein showed substantial female-specificity (Fig. 1e and Extended Data Fig. 2d–f) and predominant enrichment in the antennae and wings (Fig. 1f and Extended Data Fig. 2g). By contrast, the non-sex-specific CYP4G19, a P450 involved in the final oxidative decarbonylation step of hydrocarbon biosynthesis[16] (Extended Data Fig. 1), was very abundant in the abdominal integument but not detected in the antennae and wings of both sexes (Fig. 1f). These results indicate that *CYP4PC1* is a strong candidate for controlling CSP production, possibly the hydroxylation step.

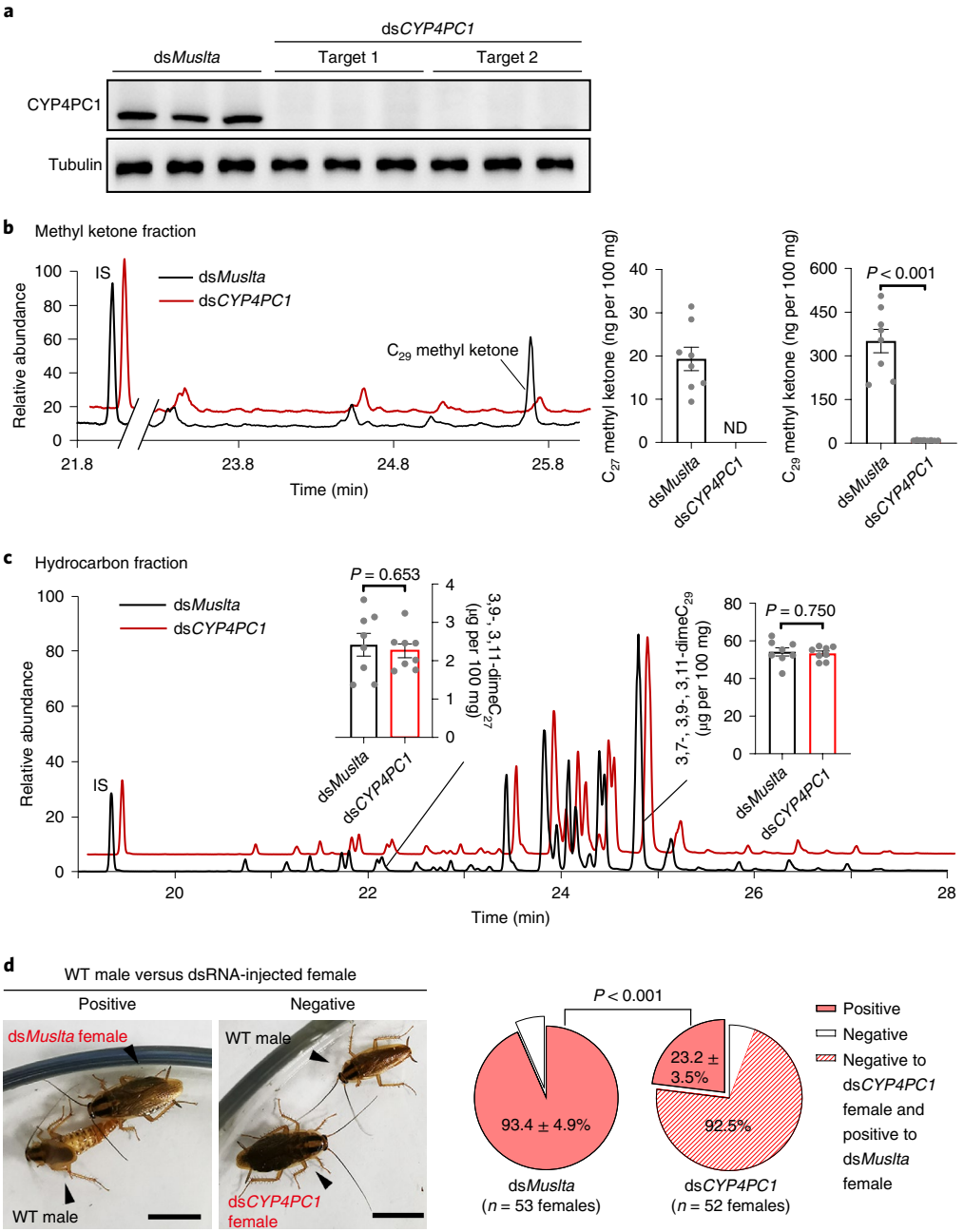

Fig. 2 | *CYP4PC1* controls female-specific CSP production and sexual attractiveness. a, Depletion of CYP4PC1 protein level in the female antennae by RNAi from the onset of N6. **b**,**c**, Effect of *CYP4PC1* knockdown (target 2) on the methyl ketone (**b**) and hydrocarbon (**c**) fractions in adult females. IS, internal standard of 14-heptacosanone in **b** and *n*-hexacosane in **c**. $n = 8$ biological replicates. ND, not detected. **d**, Behavioural phenotype (left) and percentage of wing-raising (right) in WT males in response to ds*Muslta*- and ds*CYP4PC1*-treated females. Scale bars, 1 cm. $n = 53$ (ds*Muslta*) and 52 (ds*CYP4PC1*) cockroaches from five behavioural replicates. See Supplementary Videos 1–3 for behavioural details. *P* values were determined by two-tailed unpaired *t*-test (**b**–**d**). Data in **b**–**d** are mean ± s.e.m.

***CYP4PC1* is required for CSP production and female attractiveness.** To examine whether *CYP4PC1* is required for CSP biosynthesis, we conducted systemic RNA interference (RNAi) of this gene in females from the onset of the sixth instar nymph (N6) by multiple injections of *CYP4PC1* double-stranded RNA (ds*CYP4PC1*). Effectively, each of the two dsRNA fragments caused a depletion of CYP4PC1 protein in adult females (Fig. 2a), resulting in a dramatic decrease in C_{29} methyl ketone and an under-detectable level of C_{27} methyl ketone (Fig. 2b). By contrast, *CYP4PC1* knockdown had no effect on the cuticular hydrocarbon profile, including the two 3,11-dimethyl alkanes that serve as direct precursors of the methyl ketone CSP components (Fig. 2c). We then used WT males in behavioural assays in response to dsRNA-injected females. A high percentage of WT males (93.4%) displayed courtship wing-raising in response to ds*Muslta* females (RNAi control), but only 23.2% responded to ds*CYP4PC1* females. Notably, 92.5% of the males that showed no courtship behaviour to ds*CYP4PC1* females performed wing-raising display to ds*Muslta* females (Fig. 2d and Supplementary Videos 1–3). These behavioural data indicate that *CYP4PC1* is required for the production of not only the methyl ketones that we examined, but also the alcohol and aldehyde components that are derived from the methyl ketones, as each of the

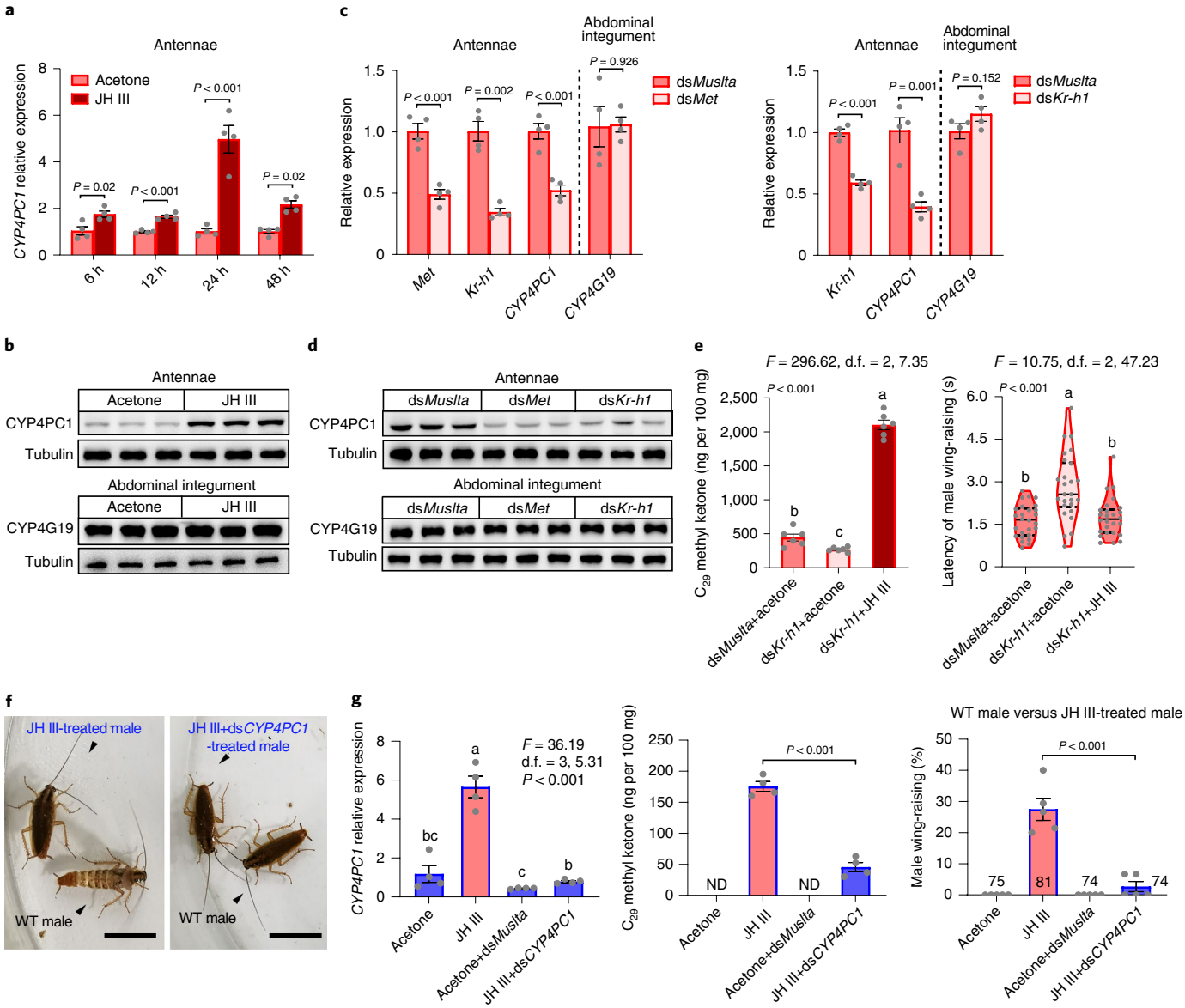

Fig. 3 | Hormone-regulated *CYP4PC1* expression sustains female attractiveness. a, *CYP4PC1* expression in the female antennae after a single JH III treatment on day 3. $n = 4$ biological replicates. **b**, CYP4PC1 and CYP4G19 protein levels in adult females 48 hours after a JH III treatment. **c**,**d**, Relative expressions of *CYP4PC1* and *CYP4G19* in females on day 5 after knockdown of *Met* or *Kr-h1* (**c**), and the effects on their protein levels on day 7 (**d**). $n = 4$ biological replicates. **e**, C_{29} methyl ketone production (left, $n = 6$ biological replicates) in females with *Kr-h1* knockdown and in those with ds*Kr-h1* and JH III treatments, and the latency of male wing-raising responses to these females (right, $n = 26$ cockroaches). The solid and dashed lines within the violin plots indicate medians and quartiles, respectively. **f**, Wing-raising courtship elicited in a WT male by a JH III-treated male but not by a male treated with both JH III and ds*CYP4PC1*. Scale bars, 1 cm. See Supplementary Video 4 for behavioural details. **g**, *CYP4PC1* expression and C_{29} methyl ketone production (both $n = 4$ biological replicates), and the percentage of WT males displaying wing-raising in JH III-treated males and those treated with both JH III and ds*CYP4PC1*. The numbers of tested males from five behavioural replicates are indicated at the bottom of the bars. ND, not detected. *P* values were determined by two-tailed unpaired *t*-test (**a**,**c**,**g**). Different letters indicate significant differences between groups using Welch's ANOVA (Games–Howell multiple comparisons test, $P < 0.05$) (**e**,**g**). Data in bar plots are mean ± s.e.m.

CSP components can independently elicit wing-raising courtship in males[8]. Furthermore, knockdown of *CYP4PC1* only in adults also remarkably reduced methyl ketone production (Extended Data Fig. 3a,b). Although the percentage of males that were stimulated to wing-raise was not affected, the latency of male wing-raising increased from 1.7 to 3.1 seconds, showing compromised female attractiveness (Extended Data Fig. 3c). In addition, *CYP4G19* knockdown in females from the onset of N6 significantly decreased the amounts of cuticular hydrocarbons and methyl ketone CSPs (Extended Data Fig. 4a,b), while injection of dsRNA against two other *CYP* genes (*C0J52_06748* and *C0J52_20733*), which showed expression patterns similar to *CYP4PC1* (Supplementary Table 1), did not alter C_{29} methyl ketone production (Extended Data Fig. 4c). These outcomes demonstrate that *CYP4PC1* is essential for CSP production that stimulates males to court females, most likely by participating in the hydroxylation of hydrocarbon precursors to CSP components.

JH-stimulated *CYP4PC1* expression sustains female attractiveness. In most adult insects including cockroaches, JH is produced

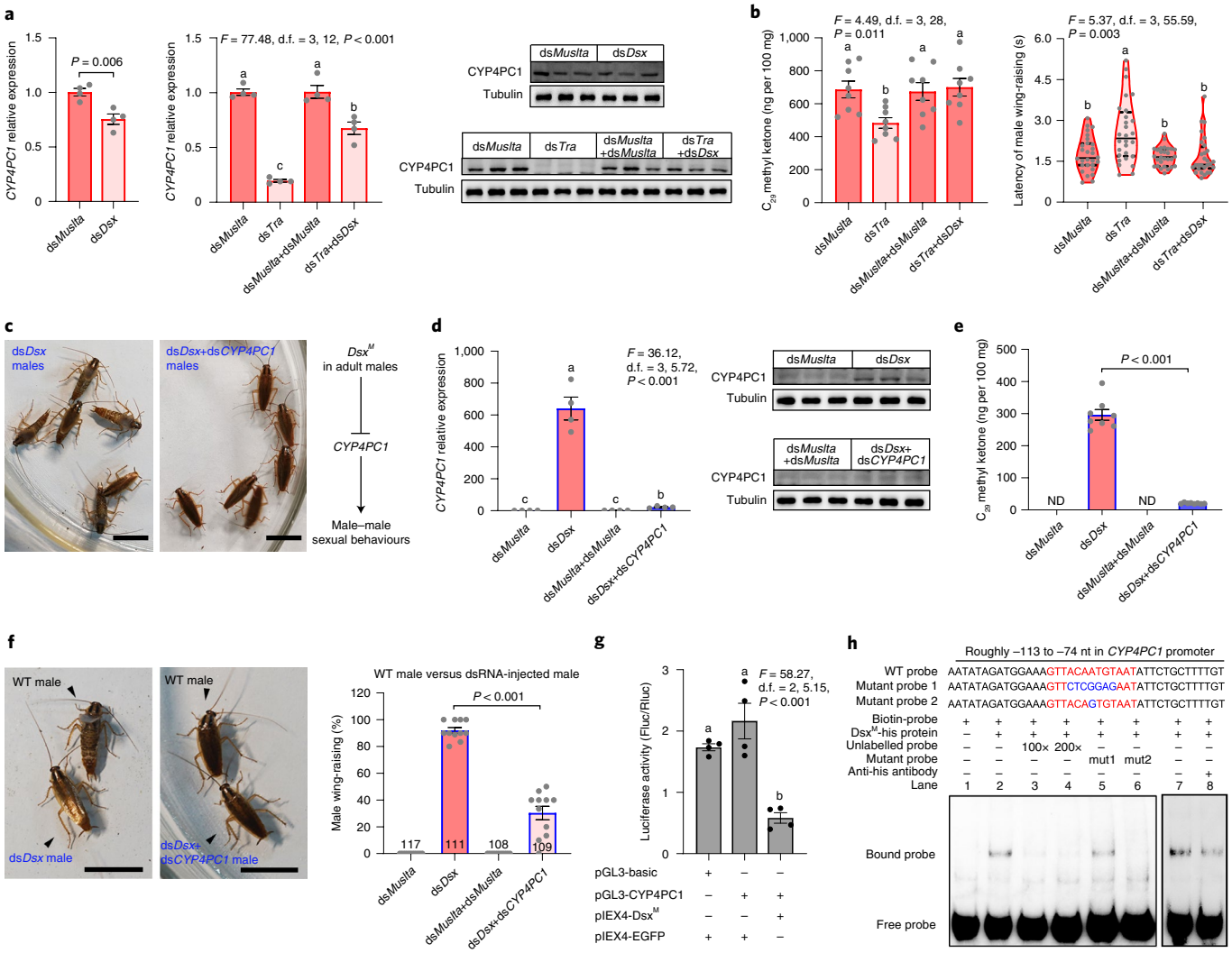

Fig. 4 | Sex differentiation genes control sexually dimorphic *CYP4PC1* expression. a, Effects of injecting ds*Dsx* or ds*Tra* alone and their coinjection on *CYP4PC1* mRNA ($n = 4$) and protein levels. **b**, The amounts of C_{29} methyl ketone pheromone in ds*Tra*-treated adult females and those with coinjection of ds*Tra* and ds*Dsx* (left, $n = 8$ biological replicates), and the effects of these treatments on the latency of wing-raising in WT males (right, $n = 28$ cockroaches per treatment). The solid and dashed lines within the violin plots indicate medians and quartiles, respectively. **c**, Homosexual behaviour in ds*Dsx*-treated males but not in males treated with both ds*Dsx* and ds*CYP4PC1*. Scale bars, 1 cm. See Supplementary Video 5 for behavioural details. **d**,**e**, *CYP4PC1* mRNA ($n = 4$ biological replicates) and protein levels (**d**), and C_{29} methyl ketone production (**e**, $n = 8$ biological replicates) in ds*Dsx*-treated males and those treated with both ds*Dsx* and ds*CYP4PC1*. ND, not detected. **f**, Behavioural phenotype and quantification of wing-raising display in WT males in response to ds*Dsx*-treated males and to males with simultaneous knockdown of *dsx* and *CYP4PC1*. The numbers of tested males from 11 behavioural replicates are indicated at the bottom of the bars. Scale bars, 1 cm. **g**, Effect of dsx^M overexpression in Kc cells on luciferase activity driven by a *CYP4PC1* promoter region (−175 to −1 nt). The pGL3-basic empty vector and pIEX4-EGFP were used as negative controls. $n = 4$ biological replicates. **h**, EMSA using in vitro translated His-tagged Dsx^M protein incubated with biotin-labelled *CYP4PC1* probe, and additional unlabelled probes (WT and mutant) or His antibody. All the probes were derived from the −113 to −74 nt *CYP4PC1* promoter region containing a putative DBS (in red), and the mutant nucleotides are marked in blue. *P* values were determined by two-tailed unpaired *t*-test (**a**,**e**,**f**). Different letters indicate significant differences determined by one-way ANOVA (Tukey HSD multiple comparisons test, $P < 0.05$) (**a**,**b** left) or Welch's ANOVA (Games–Howell multiple comparisons test, $P < 0.05$) (**b** right, **d**,**g**). Data in bar plots are mean ± s.e.m.

cyclically in females and females have a higher JH titre than males[17]. JH also regulates and coordinates reproductive maturation of the ovaries[18–20] and often sex pheromone production[5,21]. On JH binding, the JH receptor methoprene-tolerant (Met) and the coactivator Taiman (Tai) induce expression of JH primary-response genes, that is *Krüppel homologue 1* (*Kr-h1*)[17,22]. We next confirmed whether *CYP4PC1* is the putative JH-stimulated *CYP* gene in the CSP biosynthetic pathway[13]. Throughout N6 and the adult stage, *CYP4PC1* exhibited an expression pattern similar to *Kr-h1* in a sexually dimorphic manner (Extended Data Fig. 5a). Treatment of young adult females with JH III (the native JH in cockroaches) caused significant upregulation in both mRNA and protein levels of *CYP4PC1*, but not in those of *CYP4G19* (Fig. 3a,b and Extended Data Fig. 5b,c). By contrast, RNAi knockdown of either *Met* or *Kr-h1* had opposite effects on *CYP4PC1*, whereas *CYP4G19* was not affected (Fig. 3c,d and Extended Data Fig. 5d). Moreover, *Kr-h1* knockdown resulted in a decrease in C_{29} methyl ketone and consequently an increase in the latency of male wing-raising, both of which were rescued by exogenous JH III treatment (Fig. 3e and Extended Data Fig. 5e).

Since JH titre are very low in adult male cockroaches[23], we next asked whether exogenous JH application in males might emulate the effects of endogenous JH in females. We found that 27.5% of the JH III-treated adult males elicited wing-raising in WT males, a behaviour that is typically stimulated by antennal contact with females (Fig. 3f,g and Supplementary Video 4). Likewise, exogenous JH III treatment promoted substantial, although limited, *CYP4PC1* expression and C_{29} methyl ketone production in adult males (Fig. 3g and Extended Data Fig. 5f). Moreover, the JH III-induced *CYP4PC1* expression, C_{29} methyl ketone production and homosexual courtship in adult males were suppressed by *CYP4PC1* knockdown (Fig. 3g). Both loss-of-function studies in females and gain-of-function studies in males demonstrate that JH-induced *CYP4PC1* expression sustains CSP production and thus sexual attractiveness.

Sex differentiation genes control sexually dimorphic *CYP4PC1* expression. A long-standing question in the development of sexual attraction is why sex pheromones are produced in a sexually dimorphic manner. Sex differentiation genes play a key role in regulating *D. melanogaster* sex pheromone production in females[24,25], and sex pheromone reception and courtship behaviour in males[6,26,27]. We therefore examined whether female-specific *CYP4PC1* expression was controlled by sex differentiation genes. In the German cockroach, there are two female-specific *doublesex* isoforms (dsx^F; *dsx2* and *3*) and one male-specific *dsx* isoform (dsx^M; *dsx1*) (Extended Data Fig. 6a), which are controlled by an RNA splicing factor, *transformer* (*tra*), that functions in females[28]. Injection of ds*Dsx* against all isoforms into adult females only eliminated expression of *dsx2* but not *dsx3* in the antennae (Extended Data Fig. 6b), resulting in a minor decrease in *CYP4PC1* expression yet no change in its protein level (Fig. 4a). Consistent with previous studies[11,28], RNAi knockdown of *tra* in females prevented dsx^F (both *dsx2* and *3*) formation and promoted transcription of the default dsx^M (Extended Data Fig. 6c). *Tra* knockdown reduced *CYP4PC1* expression by more than 80% in the female antennae, which is much stronger than knockdown of dsx^F alone. The ds*Tra*-inhibited *CYP4PC1* mRNA and protein levels were markedly rescued by coinjection of ds*Tra* and ds*Dsx* (Fig. 4a), which resulted in depletion of both dsx^F and dsx^M (Extended Data Fig. 6d), suggesting that the concomitant ds*Dsx* removed the inhibition of *CYP4PC1* expression by ds*Tra*-induced dsx^M. Moreover, *tra* knockdown decreased C_{29} methyl ketone production and consequently prolonged the latency of male wing-raising, both of which were rescued by the simultaneous knockdown of *tra* and *dsx* (Fig. 4b). To understand whether dsx^F and dsx^M regulate *CYP4PC1* expression differently, we performed RNAi of dsx^M in adult males (Extended Data Fig. 7a, upper). Most of the ds*Dsx*-injected males courted each other with wing-raising, feeding on the tergal secretions and even attempted to copulate with other males (Supplementary Video 5), whereas these behavioural characteristics of male–male sexual attraction were completely absent in males that were simultaneously injected with ds*Dsx* and ds*CYP4PC1* (Fig. 4c). Meanwhile, dsx^M knockdown promoted substantial *CYP4PC1* mRNA and protein levels, C_{29} methyl ketone production, and sexual attractiveness to WT males, all of which were restored to low levels by *CYP4PC1* knockdown (Fig. 4d–f and Extended Data Fig. 7a, lower, 7b). By contrast, manipulation of sex differentiation pathways in both sexes did not affect CYP4G19 protein level (Extended Data Fig. 7c). These functional studies demonstrate a crucial role of sex differentiation genes in regulating sexually dimorphic *CYP4PC1* expression and thus CSP production.

In addition, RNAi knockdown of *fruitless* (*fru*), another sex differentiation gene under the control of *tra*[29], did not alter the expressions of dsx^M and *CYP4PC1* in adult males (Extended Data Fig. 7d). Considering these functional studies in both females and males, it is reasonable to assume that dsx^M should be a primary repressor for controlling sex-specific *CYP4PC1* expression. In the 5′-flanking promoter sequence of *CYP4PC1*, there exists a putative *dsx* and *mab-3*-related transcription factor binding site (DBS) located at nucleotides −99 to −87. Overexpression of dsx^M in *Drosophila* Kc cells significantly reduced the luciferase activity driven by a 175 bp *CYP4PC1* promoter fragment containing the DBS (Fig. 4g). The Dsx^M protein harbouring a His tag was translated in vitro, and we performed electrophoretic mobility shift assays (EMSA) to determine whether Dsx^M binds to the DBS. The biotin-labelled probes, derived from nucleotides −113 to −74 of the *CYP4PC1* promoter, were capable of binding Dsx^M (lane 2) and the band could be competitively eliminated by adding into the reaction 200-fold molar excess of unlabelled probes (lane 4), but not the core 7-base-mutated probes (lane 5). In addition, preincubation of the protein with a His antibody decreased the band intensity (lane 7 and 8) (Fig. 4h). Collectively, Dsx^M binds to DBS in the *CYP4PC1* promoter, thus switching off *CYP4PC1* expression in males, which precludes the production of female CSP and averts male–male sexual attraction.

Sex differentiation and JH signalling coordinately regulate CSP production. Hitherto, it is unknown whether and how sex differentiation and JH signalling pathways coordinately control any sexual signals in insects. In cockroaches, the last two steps of JH III biosynthesis are catalysed by two crucial enzymes, JH acid methyltransferase (Jhamt) and methyl farnesoate epoxidase (CYP15A1) in the corpora allata, resulting in female-biased JH III production[23,30]. RNAi knockdown of either *tra* or dsx^F caused decreases in *Jhamt* and *CYP15A1* expressions, and *tra* knockdown also downregulated *Kr-h1* in the antennae (Fig. 5a). These data indicate that sex differentiation genes regulate the expression of JH biosynthesis genes and thus JH signalling in adult females. Consistent with our previous study[19], inhibition of JH signalling reduced the expression of dsx^F but not *tra* (Fig. 5b). The crosstalk between sex differentiation and JH signalling pathways reveals that, with regard to *CYP4PC1* expression, the two pathways reciprocally magnify each other in females. Since *tra* knockdown affected JH biosynthesis, we simultaneously altered JH signalling by treatment with exogenous JH III or RNAi knockdown of *Kr-h1*. JH III treatment dramatically increased CYP4PC1 protein level, and the ds*Tra*-decreased CYP4PC1 was partially rescued by JH III treatment (Fig. 5c). Compared with RNAi knockdown of *tra* or *Kr-h1* alone, codepletion of *tra* and *Kr-h1* resulted in greater downregulation of *CYP4PC1* expression and C_{29} methyl ketone production (Fig. 5d). These experimental data confirm that sex differentiation and JH signalling coordinately regulate *CYP4PC1*-specified CSP production.

To address the question why cockroach males do not synthesize female-like CSP, even though they synthesize considerable amounts of hydrocarbon precursors of CSP, we also examined the interaction of sex differentiation and JH signalling pathways on female CSP production in adult males. RNAi knockdown of dsx^M only slightly upregulated *Jhamt*, but not *CYP15A1* and *Kr-h1*, while JH III treatment just slightly induced dsx^M expression (Fig. 5e). Simultaneous dsx^M knockdown and JH III treatment had much greater stimulatory effects than each alone on *CYP4PC1* expression and C_{29} methyl ketone production (Fig. 5f). The genetic interaction experiments demonstrate that both direct inhibition of *CYP4PC1* expression by Dsx^M binding in the promoter and the lack of JH signalling account for the absence of *CYP4PC1* expression and CSP production in adult males, and that experimentally elevated *CYP4PC1* expression is able to cause male–male sexual attractiveness and courtship behaviour.

***CYP4PC1* controls mate choice in a dose-dependent manner.** These behaviour assays suggest that by promoting female-specific CSP production, *CYP4PC1* quantitatively controls sexual recognition and attractiveness. To understand how *CYP4PC1* intercedes in mate choice, we performed competitive courtship assays, in which courtship behaviour of a single WT male was assessed in response

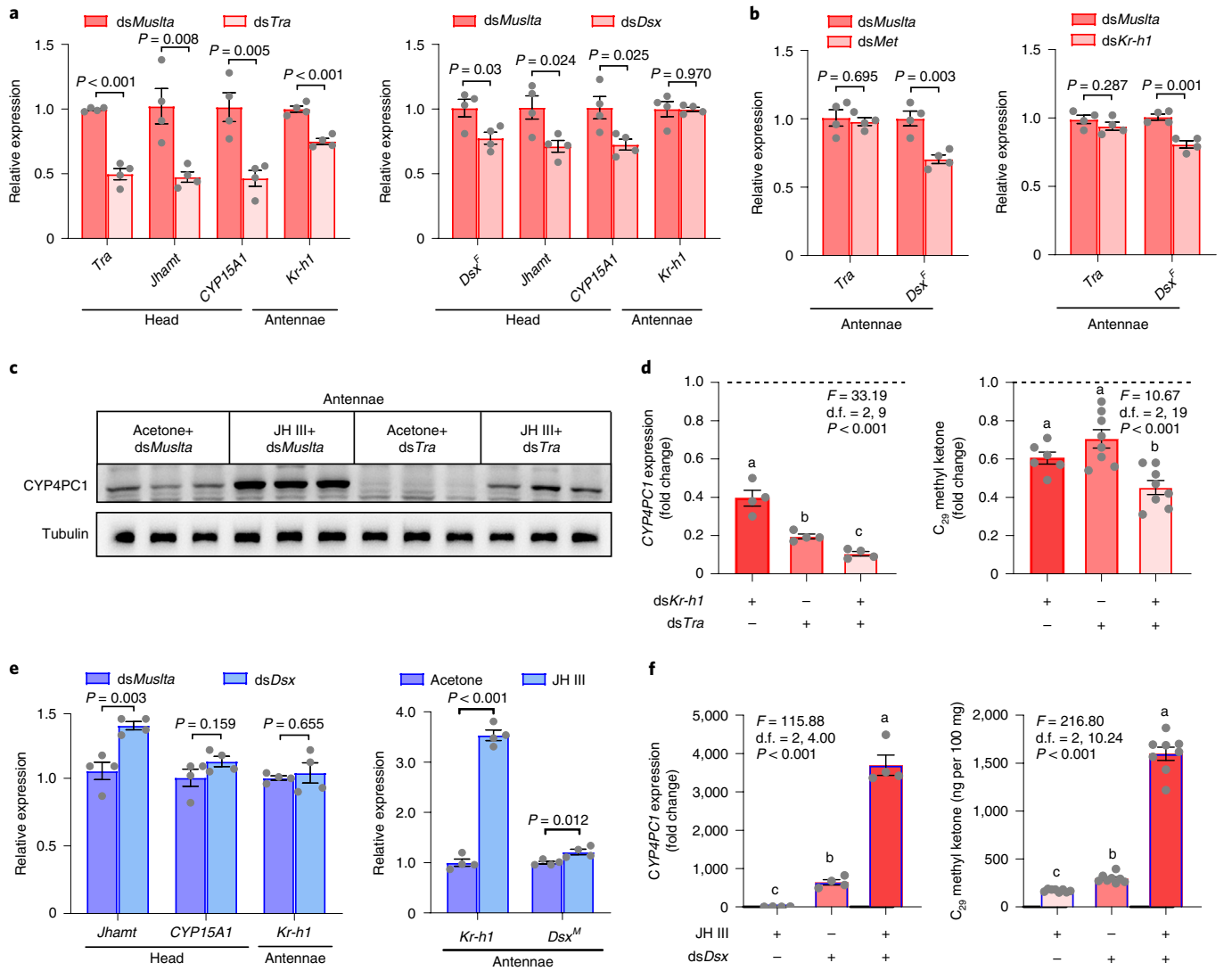

Fig. 5 | Sex differentiation and hormone signalling orchestrate *CYP4PC1*-specified sexual attractiveness. a, Downregulations of *Jhamt* and *CYP15A1* in the head, and *Kr-h1* in the antennae by RNAi knockdown of *tra* or *dsx* in adult females. $n = 4$ biological replicates. **b**, Downregulation of *dsx* but not *tra* in the antennae by RNAi knockdown of *Met* or *Kr-h1* in adult females. $n = 4$ biological replicates. **c**, Effect of *tra* knockdown in adult females on CYP4PC1 protein level in the presence of JH III. **d**, Synergistic effects of *Kr-h1* and *Tra* knockdown in adult females on *CYP4PC1* expression and C_{29} methyl ketone production. The fold change was defined as each of the data points divided by the mean of the control. $n = 4$ (left), 6 (right, ds*Kr-h1*) and 8 (right, ds*Tra* and ds*Kr-h1* + ds*Tra*) biological replicates. **e**, Effect of *dsx* knockdown in adult males on *Jhamt*, *CYP15A1* and *Kr-h1* expressions, and effect of JH III on dsx^M expression. $n = 4$ biological replicates. **f**, Synergistic effects of JH III treatment and *dsx* knockdown in adult males on *CYP4PC1* expression and C_{29} methyl ketone production. $n = 4$ (left) and 8 (right) biological replicates. *P* values were determined by two-tailed unpaired *t*-test (**a**,**b**,**e**). Different letters indicate significant differences determined by one-way ANOVA (Tukey HSD multiple comparisons test, $P < 0.05$) (**d**) or Welch's ANOVA (Games–Howell multiple comparisons test, $P < 0.05$) (**f**). Data in bar plots are mean ± s.e.m.

to two competing cockroaches (female and/or male) harbouring different *CYP4PC1* expression and CSP production. We quantified the male's courtship response with a courtship index derived from the duration of wing-raising, which was highly sensitive to CSP. A series of competitive assays demonstrated that N6 females were the least attractive to WT males, followed by increased attractiveness of adults from day 1 females. ds*Dsx*-treated day 5 males and day 5 females that were treated with both ds*Tra* and ds*Kr-h1* were similarly attractive to WT males, followed by day 5 females; day 5 males that were treated with both ds*Dsx* and exogenous JH III were most attractive (Fig. 6a). Furthermore, positive correlations between *CYP4PC1* expression and CSP production, and between CSP production and male courtship index, demonstrate that the higher *CYP4PC1* expression, the higher CSP production and thus the greater sexual attractiveness to WT males (Fig. 6b and Extended Data Fig. 8a). In conclusion, WT males prefer to court cockroaches with higher *CYP4PC1* expression and CSP production in a dose-dependent manner, regardless of the sex of the cockroach that produces the CSP. By mutually affecting each other and functioning together, sex differentiation and JH signalling orchestrate *CYP4PC1*-specified female sexual attractiveness (Fig. 6c and Extended Data Fig. 8b).

Discussion

Characterizing the key genes that control sexual signals is crucial to understand the genetic basis of sexual communication in animals, and our findings conclusively provide an insect example in which a single gene (*CYP4PC1*) integrates upstream regulators (that is,

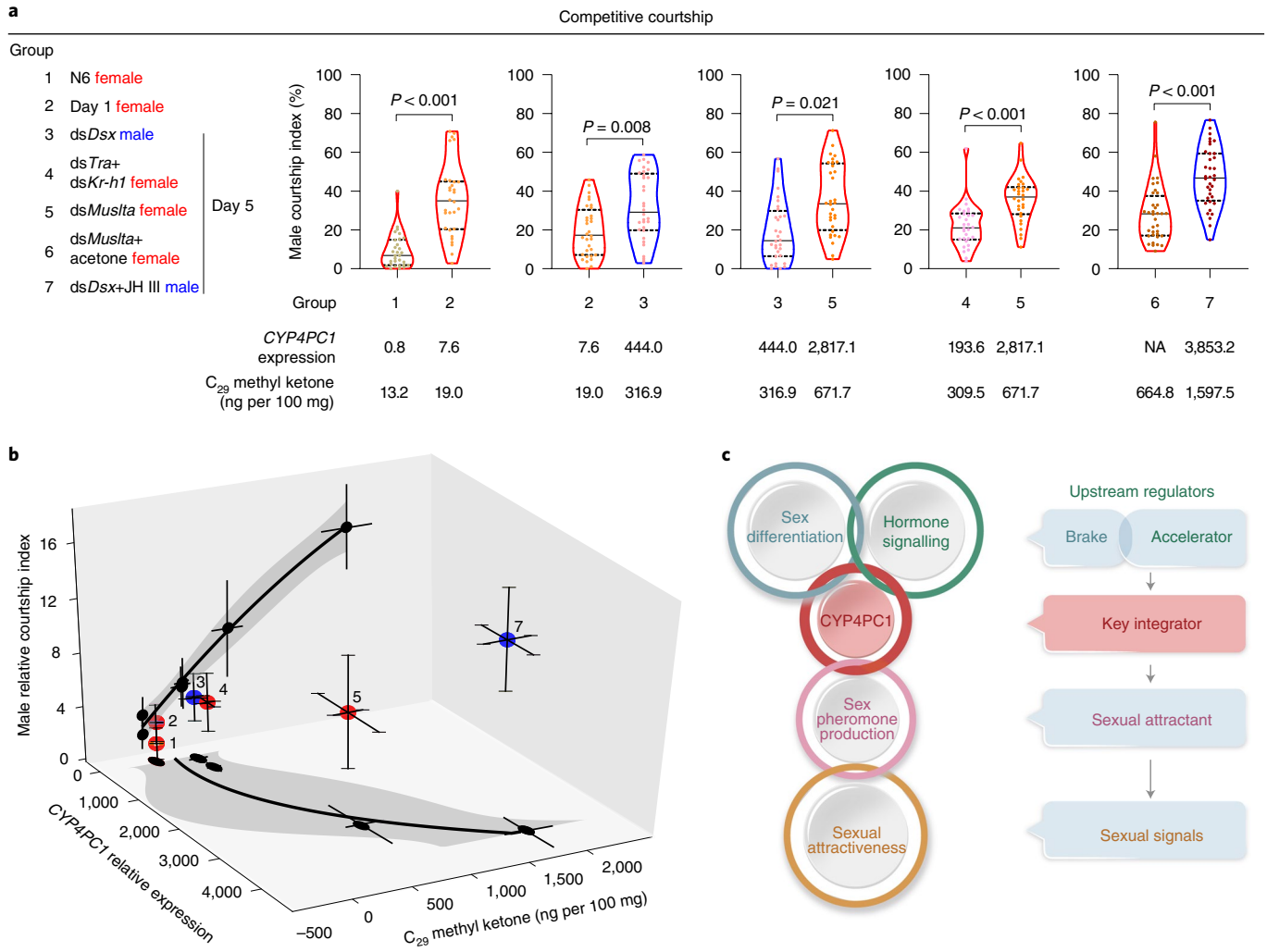

Fig. 6 | *CYP4PC1* controls mate choice in a dose-dependent manner. a, Courtship index of WT males in response to two attractive cockroaches with different *CYP4PC1* expression in a competitive courtship assay. The solid line and dashed lines within each violin plot indicate median and quartiles, respectively. NA, not applicable. *P* values were determined by a two-tailed paired *t*-test. **b**, Non-linear curve fitting between *CYP4PC1* expression and CSP production, and between CSP production and male courtship index. The 95%CI is indicated by the grey area. The source data are derived from groups 1–5 and 7 in **a**. Data are mean ± s.d. **c**, A summary model highlighting a key integrator role of *CYP4PC1* that links upstream regulators with CSP production and thus sexual attractiveness in cockroaches. The sex differentiation gene dsx^M functions as a brake of *CYP4PC1* expression in males, and JH signalling plays an accelerator role during sexual maturation in females.

sex differentiation and hormone signalling) with female-specific pheromone production that stimulates courtship in males (Fig. 6c). Comprehensive data from RNA screening, expression profiling and functional studies reveal that *CYP4PC1* encodes the rate-limiting hydroxylase for CSP production in females. Unlike a previous report claiming that the abdominal integument is a major site for CSP production[15], we found that the antennae and wings had considerably higher relative *CYP4PC1* expression and C_{29} methyl ketone concentration (ng mg^{-1} tissue mass). The enrichment of CSP on the antennae and wings matches well with the courtship sequence, where males perform antennal 'fencing' to recognize and assess females primarily via her antennae and wings. Since hydrocarbon biosynthesis is specific to clustered oenocytes underneath the abdominal integument[15,16,31], it is very likely that the 3,11-dimethyl alkane precursors are primarily transported from oenocytes to the antennae and wings, in which functional CSP components are produced through female-specific hydroxylation by CYP4PC1 and subsequent oxidation.

The regulatory mechanisms of *CYP4PC1* expression confirm its rate-limiting role in CSP production. Our genetic interaction data demonstrate that dsx^M prevents *CYP4PC1* expression in males by physically binding the DBS in the *CYP4PC1* promoter, whereas *tra* in females removes this inhibition by directing female-specific splicing of *dsx* (dsx^F). Then, JH is capable of promoting *CYP4PC1* expression and CSP production, both of which reach high levels in sexually mature females. Such a mechanism enables the production of sex-specific signals only in females (dsx^M-free, no brake) on maturation (high JH, accelerator), but not in males (dsx^M, brake; low JH, no accelerator) (Extended Data Fig. 8b). CSP production and sexual attractiveness, which are coordinately regulated by both sex differentiation and JH signalling either developmentally or experimentally in the adult stage, can be abolished by *CYP4PC1* knockdown, indicating that *CYP4PC1* (key integrator) is central to the genetic connections between upstream regulators and sexual attractiveness. The model of such key genes integrating sex and hormone regulators may well apply to other insects that show similar pathways

for controlling sex-specific pheromone production[5,25], and probably other sexual signals. Compared with the limited induction of CSP production by exogenous JH III in males, the *dsx*^{M}-depleted males are fully capable of eliciting courtship from males, thus highlighting the direct inhibition of *CYP4PC1* expression by Dsx^{M} binding in the promoter. Together with the studies on mammals in which sex differentiation is often manifested by sex steroid hormones after gonad development[32], it appears that coordinate regulation of sexual signals and attractiveness by sex differentiation and hormone signalling could be universal across insects and other taxa.

Methods

Animals. The line of *B. germanica* was a well-established laboratory strain originally collected from downtown Shanghai in the 1970s[11,16]. Cockroaches were kept in plastic jars on egg cartons at 27 °C, with a 70% relative humidity and a 12:12 h light/dark photoperiod. They were provided with commercial rat chow and tap water. For harvesting pools of synchronized cockroaches, newly hatched nymphs during a 24-h period were collected and cultured in new jars. Freshly emerged nymphs and adults were separated from the colony by sex on the day of moulting (day 0) and maintained in groups.

Chemicals. Gas chromatography-grade *n*-hexane was purchased from Aladdin Biochemical Technology (no. H100107). C_7–C_{40} saturated *n*-alkanes (no. 49452-U) and *n*-hexacosane (no. 52183) standards were purchased from Sigma-Aldrich. 14-heptacosanone standard was obtained from TCI Shanghai Chemical (no. H0512). JH III was purchased from Cayman Chemical (no. 19646). Other chemicals and organic solvents were analytical grade unless otherwise specified.

RNA-seq and assembly. The antennae and abdominal integuments were dissected from adult cockroaches under the protection of RNAlater solution (no. AM7021, Thermo Fisher Scientific Baltics UAB). Total RNA isolation and digestion of genomic DNA were conducted with a Direct-zol RNA Miniprep Kit (no. R2072, Zymo Research). The obtained complementary DNA libraries were sequenced on Illumina Novaseq6000 platform at Biomarker Technologies (antennae samples) and Illumina HiSeq2000 platform at Whbioacme Co., Ltd (abdominal integument samples). After quality evaluation and removal of the redundant sequences, the clean reads were mapped to the *B. germanica* genome[14] using Hisat2 software. Gene expression level is presented as fragments per kilobases of transcript per million mapped reads (FPKM) (Supplementary Tables 1 and 2). For acquisition of protein-coding gene sequences, de novo assembly of the clean reads was generated by using the Trinity program with default parameters.

5′ Rapid amplification of cDNA ends (5′ RACE). The SMARTer RACE 5′/3′ Kit (no. 634859, Takara) was used to generate RACE libraries with antennal RNA from sexually mature females. The 5′-RACE-Ready cDNA was synthesized from 1 μg of total RNA using the SMARTScribe Reverse Transcriptase. 5′ RACE was first performed with a gene-specific primer (Supplementary Table 3) and the kit-provided universal primer mix and SeqAmp DNA polymerase. This amplification was controlled by a touchdown PCR thermocycling program as described in the supplier's manual. Using 1:200 diluted PCR product as a template, a nested PCR was then performed with a nested gene-specific primer and the universal primer mix under 25 cycles of 94 °C for 30 s, 68 °C for 30 s and 72 °C for 2 min. The PCR products were gel-purified and cloned into a pTOPO-Blunt Vector (no. CV2101, Aidlab Biotech.). The sequences from 12 clones were aligned to obtain the 5′ untranslated region sequence.

Reverse transcription PCR and qPCR. Total RNA was extracted from a pool of tissues or body parts (15 pair of antennae, eight pairs of wings, eight heads, five guts, five abdominal integuments, three thoraxes, 18 legs from three cockroaches, three pairs of ovaries and fat body from three insects) as described elsewhere, and 2 μg of the RNA extracts was primed with oligo(dT)s and reverse-transcribed to first-strand cDNA with Reverse Transcription M-MLV (RNase H-) (no. 2641A, Takara). For validation of substantial *CYP4PC1* transcript, the full length coding sequence (CDS) was amplified from various tissues using Takara LA Taq (no. RR02MA).

For qPCR analysis, standard curves were established with diluted cDNA gradients to screen specific primer pairs with an efficiency ranging from 0.90 to 1.05. All qPCR analyses were performed with biological replicates, each with technical triplicates, on a QuantStudio 6 Flex Real-Time PCR system (Life Technologies Holdings Pte. Ltd.). The volume of each reaction was 20 μl including 10 μl of Hieff qPCR SYBR Green Master Mix (no. 11202ES08, Yeasen), 8 μl of 20-fold diluted cDNA and 1 μl of each forward and reverse primer. The thermocycling was initiated from 94 °C for 3 min, followed by 40 cycles of 94 °C for 10 s and 56 °C for 30 s. The *actin-5c* gene was used as an endogenous control for normalization[29,33,34]. All primer sequences used in this study are summarized in Supplementary Table 3.

RNAi in vivo. *RNAi construction and dsRNA preparation.* For RNAi-mediated knockdown of different target genes in *B. germanica*, gene-specific fragments of each open reading frame were PCR amplified with Takara Ex Taq (no. RR001A) or PrimeSTAR HS DNA Polymerase (no. DR010A). RNAi constructs of *CYP4G19* and *Mus musculus lymphotoxin A* (*Muslta*, RNAi control) have been reported in our previous study[16]. The DNA fragments for RNAi constructs of *Met*, *Kr-h1*, *Tra*, *Dsx* and *Fru* were selected as described elsewhere[28,29,33,34] and summarized in Supplementary Table 3. For knockdown of *CYP4PC1*, we amplified two distinct fragments, one 374 bp (target 1) and the other 323 bp (target 2), as dsRNA templates. All these fragments were cloned into either a pGEM-T Easy Vector (no. A1360, Promega) or a pTOPO-Blunt Vector (Aidlab Biotech.), and were validated by Sanger-based DNA sequencing (Tsingke). The T7 promoter sequence-attached primer pairs together with the verified plasmids were used to generate template fragments for dsRNA synthesis[16,18]. The dsRNA was synthesized and purified in accordance with the T7 RiboMAX Express RNAi kit (no. P1700, Promega). All dsRNAs were separated into aliquots and preserved at −80 °C before microinjection.

Delivery of dsRNA by microinjection. We adopted a strategy of multiple injections of dsRNA for effective gene knockdown. In separate experiments, dsRNA injections were initiated from either N6 or in adults. Cockroaches were briefly anaesthetized with carbon dioxide, and 2 μl of dsRNA was injected into the haemocoel through the fourth abdominal intersegmental membrane. All injections were implemented using a NanoFil 10 μl syringe (35G bevelled needle, World Precision Instruments) interfaced with an ALC-IP600 precision syringe pump (Alcott Biotech.) under the view of a light microscope. For cockroaches at N6, two injections of dsRNA, each with 3 μg, were performed on day 1 and day 6, and for adults, two injections, each with 6 μg, were performed on day 0 and day 3. In terms of RNAi knockdown of *Met* and *Kr-h1* in adults, we used a dose of 12 μg for each injection. Control groups received the same dose of dsRNA specific to *Muslta*.

JH treatment. Adult cockroaches were briefly anaesthetized with carbon dioxide, and 1 μl of JH III solution (10 or 20 μg μl^{-1} in acetone) was topically applied on the prosternum with a manual syringe[33]. To investigate whether *CYP4PC1* and *CYP4G19* transcripts are induced by JH in adult females, we performed a single application of 20 μg JH III on day 3. For testing the potential of JH to promote *CYP4PC1* expression and CSP production in adult males, three applications of JH III, each with 20 μg, were performed on days 1, 3 and 5.

Genetic interaction experiments. To explain the genetic network that regulates sexually dimorphic *CYP4PC1* expression, we adopted double RNAi knockdown and simultaneous RNAi and JH application in both adult males and females. The same dose of ds*Muslta* was used as a negative control for RNAi, and acetone application was used as negative control for JH treatment.

Genetic interactions within a signalling cascade. For restoring JH signalling after *Kr-h1* knockdown in females, a dose of 20 μg JH III was applied on the day of the second injection of dsRNA (day 3). For RNAi knockdown of *CYP4PC1* after JH induction in males, a single injection of dsRNA was performed on the day of the second JH application (day 3). For additional knockdown of *dsx*^{M} isoform that resulted from *tra* knockdown in females, coinjection of ds*Tra* and ds*Dsx*, each with 6 μg, was performed on day 0 and day 3. Similarly in males, we simultaneously injected 6 μg of ds*Dsx* and 6 μg of ds*CYP4PC1*, on day 0 and day 3.

Genetic interactions between two signalling pathways. To investigate the effect of *tra* knockdown on *CYP4PC1* expression in the presence of JH, we applied 10 μg of JH III in parallel with dsRNA injection on day 0 and day 3. For maximum downregulation of *CYP4PC1* expression in females, simultaneous injection of ds*Tra* and ds*Kr-h1*, with 6 μg of ds*Tra* and 12 μg of ds*Kr-h1*, was performed on day 0 and day 3. Conversely, in males, we injected 6 μg of ds*Dsx* on day 0 and again on day 3, and applied 20 μg of JH III on day 1 and again on day 3, for maximum upregulation of *CYP4PC1* expression.

Antibody generation and western blotting. Rabbit polyclonal antibodies targeting either recombinant *B. germanica* CYP4PC1 or CYP4G19 peptide were prepared and purified by Wuhan GeneCreate Biological Engineering Co., Ltd. In brief, the sequence encoding the peptide of CYP4PC1 (Y27–E302) or CYP4G19 (R40-E340) was cloned into pET-B2m vector, expressed in *Escherichia coli* with 6×His tag at the N terminus. The recombinant protein was then affinity purified by Ni-chelating chromatography, and used as an antigen for raising antibody. Antibody titres from the antiserum were determined by enzyme-linked immunosorbent assay, and the antiserum with the highest titre was affinity purified with Protein G chromatography. The specificity and authenticity of the obtained antibodies were determined by western blotting and RNAi experiments. The anti-CYP4PC1 antibody recognized three primary bands between 45 and 60 kDa. Among them, an approximately 58 kDa protein was female-specific, and its level increased in the first vitellogenic cycle and decreased by *CYP4PC1* knockdown (Extended Data Fig. 2f). The antibody developed against recombinant CYP4G19 could specifically recognize endogenous CYP4G19 (62 kDa) from protein extracts of abdominal integument, and the protein level could be depleted by *CYP4G19* knockdown

(Extended Data Fig. 4a, inset). These results indicate that the two antibodies could be used to detect the target proteins in cockroach tissues.

Total protein was extracted with freshly prepared RIPA Lysis Buffer (no. P0013B, Beyotime) supplemented with 1% (v/v) phenylmethylsulfonyl fluoride. Immediately afterwards, the protein concentration was determined by Bradford protein assay. As a general guide, approximately 5 μg of protein extract was separated per lane by sodium dodecyl sulfate–polyacrylamide gel electrophoresis and then transferred to polyvinylidene difluoride membranes (no. ISEQ00010, Millipore). The tubulin protein was used as a loading control. The membranes were separately incubated at 4 °C overnight with primary antibodies against either target protein (rabbit polyclonal CYP4PC1 or CYP4G19 antibody, 1:5,000) or reference protein (mouse monoclonal antibody against tubulin, no. AT819-1, 1:5,000, Beyotime). HRP-conjugated goat antirabbit or -mouse IgG (nos. A0208 and A0216, both 1:5,000, Beyotime) was used as secondary antibody. Protein bands were finally detected by chemiluminescence using a High-Sig ECL Substrate (no. 180-501, Tanon).

Dual-luciferase reporter assay. On the basis of our 5′ RACE result, a 175 bp fragment from the *CYP4PC1* promoter region (roughly −175–−1 nt) was cloned into the *Kpn*I and *Bgl*II cleavage sites of pGL3-basic vector conjugated to firefly luciferase using a Hieff Clone Plus One Step Cloning Kit (no. 10911ES20, Yeasen). Likewise, the full length CDS of dsx^M was cloned into the *Kpn*I and *Not*I cleavage sites of pIEX4 vector (Invitrogen). The primers used for these constructions are summarized in Supplementary Table 3. The pGL3 reporter plasmid was co-transfected with the pIEX4-Dsx^M expression plasmid and a reference pGL4.73[hRluc/SV40] vector into *Drosophila* Kc cells breeding in 96-well plates. The pIEX4-EGFP vector was used as a negative control. After incubation of the cells at 28 °C for 48 h, western blotting was performed to confirm Dsx^M expression. Luciferase activity was measured using the Dual-Luciferase Reporter Assay System (no. E1960, Promega) and a GloMax 96 Microplate Luminometer (Promega)[35,36].

DNA-protein binding assay. The full length CDS of dsx^M was amplified with KOD-Plus-Neo DNA polymerase (no. KOD-401, Toyobo) from male antennal cDNAs, with a 6×His tag fused to the 3′ terminus, and cloned into the *Kpn*I and *Not*I cleavage sites of pcDNA3.1(+) (Invitrogen). An aliquot of 1 μg of the recombinant pcDNA3.1-Dsx^M was subjected to a 50-μl translation reaction using the TNT T7 Quick Coupled Transcription/Translation System (no. L1170, Promega). The reaction was incubated at 30 °C for 2 h. For confirming successful translation, 1 μl of the products was subjected to western blotting with 1:5,000 monoclonal His antibody (no. 12698S, Cell Signaling Technology).

The −113–−74 nt fragment from the *CYP4PC1* promoter region was synthesized with biotin-labelling at the 3′ terminus, followed by denaturing and annealing to generate a labelled probe. Binding reaction was performed by incubating 2 μl of translated Dsx^M product with 20 fmol of biotin-labelled probe, in a total volume of 20 μl containing 1× binding buffer, 2.5% glycerol, 5 mM $MgCl_2$, 0.05% NP-40 and 1 μg of poly(dI·dC). In the competition assays, 100- or 200-fold molar excess of unlabelled (WT or mutant) probe was added into the binding reaction. For the super-shift assay, 1 μl of His antibody was preincubated with translated Dsx^M product for 2 h at 4 °C before adding the labelled probe. All reactions were then maintained at room temperature for 20 min, and immediately separated by 6% native acrylamide gel electrophoresis. The gel was transferred onto a positively charged nylon membrane (no. INYC00010, Millipore), developed with LightShift Chemiluminescent EMSA Kit (no. 20148, Thermo Scientific) according to the manufacturer's instructions, and complexes were finally visualized via chemiluminescence[35,36]. High-performance liquid chromatography-purified oligo sequences used in EMSA experiment are listed in Supplementary Table 3.

Cuticular hydrocarbons and methyl ketone CSP chemistry. Cuticular lipids from a pool of cockroaches (three females or four males) were extracted with two 5-min hexane washes, followed by a quick wash with 1 ml of hexane[16]. Before the extraction, 30 μg of *n*-hexacosane and 500 ng of 14-heptacosanone were added as internal standards for quantification of the hydrocarbon and methyl ketone components, respectively, by gas chromatography–mass spectrometry. The hexane extracts were concentrated to roughly 300 μl with a gentle nitrogen stream, and were then loaded onto 400 mg chromatographic silica gel (no. 60741, 70–230 mesh, Sigma-Aldrich) in a glass wool-stoppered Pasteur pipette (no. 63A54, Kimble). The silica gel column was activated by heating at 110 °C for 40 min and subjected to a quick rinse with 1 ml of hexane before loading of the extracts. The hydrocarbon fraction was eluted with 10 ml of hexane, and the methyl ketone fraction was eluted with 7 ml of freshly prepared 2% diethyl ether in hexane[8].

For gas chromatography–mass spectrometry analysis, the hydrocarbon fraction was reduced to roughly 6 ml and the methyl ketone fraction was taken to dryness by a nitrogen stream and reconstituted in 100 μl of hexane. Samples were analysed using a TRACE 1310 gas chromatograph equipped with an ISQ single quadruple mass spectrometer (Thermo Scientific). Splitless injection of 1 μl of the extracts was separated by a HP-5MS UI capillary column (no. 19091S-413UI, 30 m × 0.32 mm × 0.25 μm, Agilent Technologies) programmed from 60 °C for 2 min, then ramped at 30 °C min^{-1} to 200 °C, followed by a 5 °C min^{-1} ramp to 320 °C and ending with a 10 min hold. Both the inlet temperature and transfer line were maintained at 280 °C. Mass spectrometry scanning was set in electrospray ionization mode ranging from 45–650 *m*/*z*, and the scan rate was five scans per s. Data acquisition and processing were performed using the Xcalibur v.2.2 software. Hydrocarbons and methyl ketones were identified on the basis of their diagnostic ions[16,37].

Behavioural assays. We performed a series of behavioural assays to test male courtship activity and preference in relation to female attractiveness and male–male attraction. A 12 cm diameter × 2.5 cm glass dish, with a thin layer of petroleum jelly smeared on the inner wall, was used for behavioural observation. All WT males and females used for behavioural assays were isolated by sex after the adult moult and kept in groups until use. Typical video recording and imaging of behavioural phenotype were implemented using a Lumix GH4 camera.

Single-pair courtship (male–female). To test male courtship response to females with different experimental treatments, as indicated elsewhere, we introduced a 7-day-old WT male to a treated female. The male was allowed antennal contact with the female three times. In any of the three attempts, a typical wing-raising accompanied by body rotation of the male was regarded as a positive response[38]. A single replicate consisted of 10–15 male individuals were tested with an equal number of the treated females, and 5–8 replicates were performed for each experimental treatment.

As a general guide, we first calculated the male wing-raising percentage to investigate the differences in female attractiveness between treatments. Since a wing-raising display could be fully elicited by just a few nanograms of CSP[8,38], a lack of notable difference in wing-raising percentages between treatments prompted us to use a more sensitive parameter, the latency of wing-raising, defined as the time from male antennal contact to his wing-raising display[38]. To this end, approximately 30 males (5-day-old) were tested for each group of the treated females monitored with a high-definition video recording system (Hikvision). The latency of the first wing-raising event (seconds) in each male was recorded by re-examining the source videos frame-by-frame.

Single-pair courtship followed by competitive courtship (male–female). To further examine the contribution of *CYP4PC1* knockdown in females to the male's response, we performed a competitive courtship assay immediately after the single-pair assay. After three observations of antennal contact of a WT male with a ds*CYP4PC1* female and no wing-raising display by the male, a ds*Muslta* control female was introduced into the glass dish. The percentages of males that performed wing-raising in response to ds*CYP4PC1* females and later to ds*Muslta* females were scored.

Single-pair courtship (male–male). Males do not display courtship wing-raising in response to other males. To test male courtship activity in male–male interactions, we introduced a 14-day-old WT male to a JH- or ds*Dsx*-treated male. Before the test, the wing of the WT male was marked with black paint to distinguish the two males. As described above, each WT male was allowed to contact and court a treated male three times, and the wing-raising percentage was recorded.

Competitive courtship. To test male courtship preference, we introduced a 7-day-old WT male to two differently treated cockroaches as indicated elsewhere. The male was allowed to court either of the two cockroaches, and all behaviours were monitored by a high-definition video recording system. The total duration of male wing-raising to each cockroach in the first 10 min was derived by re-examining the source videos. Male courtship index was defined as total wing-raising duration (seconds) divided by 600 (60 s × 10 min).

Data analyses and statistics. Statistical analyses were performed with the IBM SPSS Statistics v.19.0 software. All the error bars surrounding the means indicate s.e.m. or s.d. Significant differences between two independent groups were determined by two-tailed unpaired *t*-test. For comparisons of multiple treatments, we performed either one-way analysis of variance (ANOVA) followed by Tukey honestly significant difference (HSD) test (homogeneity of variances assumed) or Welch's ANOVA followed by the Games–Howell test (homogeneity of variances not assumed) at the level of $P < 0.05$. Significant differences of male courtship index values in response to the two groups in competitive courtship assays were determined by two-tailed paired *t*-test. A geno_smooth function was adopted for fitting *CYP4PC1* expression and CSP amount, as well as CSP amount and male courtship index using ggplot2 package in R. The three-dimensional graph in Fig. 6b was plotted by integrating numpy, matplotlib and mpl_toolkit packages in Python v.3.7. All other data were plotted with GraphPad Prism v.8.0.2 and formatted by Adobe Illustrator CC software.

Reporting summary. Further information on research design is available in the Nature Research Reporting Summary linked to this article.

Data availability

All data and materials generated in this study are available in the main text, supplementary materials and source data. RNA-seq data have been deposited to National Center for Biotechnology Information's Sequence Read Archive database under accession numbers PRJNA759392 and PRJNA760811. Source data are provided with this paper.

Received: 25 January 2022; Accepted: 23 May 2022;
Published online: 04 July 2022

References

1. Ryan, M. J. Darwin, sexual selection, and the brain. *Proc. Natl Acad. Sci. USA* **118**, e2008194118 (2021).
2. Le Moëne, O. & Ågmo, A. The neuroendocrinology of sexual attraction. *Front. Neuroendocrinol.* **51**, 46–67 (2018).
3. Witchel, S. F. Disorders of sex development. *Best Pract. Res. Clin. Obstet. Gynaecol.* **48**, 90–102 (2018).
4. Mäkelä, J., Koskenniemi, J. J., Virtanen, H. E. & Toppari, J. Testis development. *Endocr. Rev.* **40**, 857–905 (2019).
5. Bilen, J., Atallah, J., Azanchi, R., Levine, J. D. & Riddiford, L. M. Regulation of onset of female mating and sex pheromone production by juvenile hormone in *Drosophila melanogaster*. *Proc. Natl Acad. Sci. USA* **110**, 18321–18326 (2013).
6. Auer, T. O. & Benton, R. Sexual circuitry in *Drosophila*. *Curr. Opin. Neurobiol.* **38**, 18–26 (2016).
7. Schal, C., Fan, Y. & Blomquist, G. J. in *Insect Pheromone Biochemistry and Molecular Biology* (eds Blomquist, G. J. & Vogt, R. G.) 283–322 (Elsevier Academic Press, 2003).
8. Eliyahu, D., Nojima, S., Mori, K. & Schal, C. New contact sex pheromone components of the German cockroach, *Blattella germanica*, predicted from the proposed biosynthetic pathway. *J. Chem. Ecol.* **34**, 229–237 (2008).
9. Nojima, S., Schal, C., Webster, F. X., Santangelo, R. G. & Roelofs, W. L. Identification of the sex pheromone of the German cockroach, *Blattella germanica*. *Science* **307**, 1104–1106 (2005).
10. Mori, K. Synthesis of all the six components of the female-produced contact sex pheromone of the German cockroach, *Blattella germanica* (L.). *Tetrahedron* **64**, 4060–4071 (2008).
11. Pei, X.-J. et al. Modulation of fatty acid elongation in cockroaches sustains sexually dimorphic hydrocarbons and female attractiveness. *PLoS Biol.* **19**, e3001330 (2021).
12. Nishida, R., Fukami, H. & Ishii, S. Sex pheromone of the German cockroach (*Blattella germanica* L.) responsible for male wing-raising: 3,11-dimethyl-2-nonacosanone. *Experientia* **30**, 978–979 (1974).
13. Chase, J., Touhara, K., Prestwich, G. D., Schal, C. & Blomquist, G. J. Biosynthesis and endocrine control of the production of the German cockroach sex pheromone 3,11-dimethylnonacosan-2-one. *Proc. Natl Acad. Sci. USA* **89**, 6050–6054 (1992).
14. Harrison, M. C. et al. Hemimetabolous genomes reveal molecular basis of termite eusociality. *Nat. Ecol. Evol.* **2**, 557–566 (2018).
15. Gu, X., Quilici, D., Juarez, P., Blomquist, G. J. & Schal, C. Biosynthesis of hydrocarbons and contact sex pheromone and their transport by lipophorin in females of the German cockroach (*Blattella germanica*). *J. Insect Physiol.* **41**, 257–267 (1995).
16. Chen, N., Pei, X., Li, S., Fan, Y.-L. & Liu, T.-X. Involvement of integument-rich *CYP4G19* in hydrocarbon biosynthesis and cuticular penetration resistance in *Blattella germanica* (L.). *Pest Manag. Sci.* **76**, 215–226 (2020).
17. Roy, S., Saha, T. T., Zou, Z. & Raikhel, A. S. Regulatory pathways controlling female insect reproduction. *Annu. Rev. Entomol.* **63**, 489–511 (2018).
18. Li, S. et al. The genomic and functional landscapes of developmental plasticity in the American cockroach. *Nat. Commun.* **9**, 1008 (2018).
19. Zhu, S. et al. Insulin/IGF signaling and TORC1 promote vitellogenesis via inducing juvenile hormone biosynthesis in the American cockroach. *Development.* **147**, dev188805 (2020).
20. Luo, W. et al. Juvenile hormone signaling promotes ovulation and maintains egg shape by inducing expression of extracellular matrix genes. *Proc. Natl Acad. Sci. USA* **118**, e2014461118 (2021).
21. Tillman, J. A., Seybold, S. J., Jurenka, R. A. & Blomquist, G. J. Insect pheromones—an overview of biosynthesis and endocrine regulation. *Insect Biochem. Mol. Biol.* **29**, 481–514 (1999).
22. Jindra, M., Palli, S. R. & Riddiford, L. M. The juvenile hormone signaling pathway in insect development. *Annu. Rev. Entomol.* **58**, 181–241 (2013).
23. Piulachs, M. D., Maestro, J. L. & Belles, X. Juvenile hormone production and accessory gland development during sexual maturation of male *Blattella germanica* (L.) (Dictyoptera: Blattellidae). *Comp. Biochem. Physiol. A* **102**, 477–480 (1992).
24. Ferveur, J. F. et al. Genetic feminization of pheromones and its behavioral consequences in *Drosophila* males. *Science* **276**, 1555–1558 (1997).
25. Shirangi, T., Dufour, H., Williams, T. & Carroll, S. Rapid evolution of sex pheromone-producing enzyme expression in *Drosophila*. *PLoS Biol.* **7**, e1000168 (2009).
26. Verhulst, E. C., de Zande, L. & Beukeboom, L. W. Insect sex determination: it all evolves around *transformer*. *Curr. Opin. Genet. Dev.* **20**, 376–383 (2010).
27. Yamamoto, D. & Koganezawa, M. Genes and circuits of courtship behaviour in *Drosophila* males. *Nat. Rev. Neurosci.* **14**, 681–692 (2013).
28. Wexler, J. et al. Hemimetabolous insects elucidate the origin of sexual development via alternative splicing. *eLife* **8**, e47490 (2019).
29. Clynen, E., Ciudad, L., Belles, X. & Piulachs, M.-D. Conservation of *fruitless*' role as master regulator of male courtship behaviour from cockroaches to flies. *Dev. Genes Evol.* **221**, 43–48 (2011).
30. Defelipea, L. A. et al. Juvenile hormone synthesis: 'esterify then epoxidize' or 'epoxidize then esterify'? Insights from the structural characterization of juvenile hormone acid methyltransferase. *Insect Biochem. Mol. Biol.* **41**, 228–235 (2011).
31. Fan, Y., Zurek, L., Dykstra, M. J. & Schal, C. Hydrocarbon synthesis by enzymatically dissociated oenocytes of the abdominal integument of the German cockroach, *Blattella germanica*. *Naturwissenschaften* **90**, 121–126 (2003).
32. Beach, F. A. Sexual attractivity, proceptivity, and receptivity in female mammals. *Horm. Behav.* **7**, 105–138 (1976).
33. Lozano, J. & Belles, X. Conserved repressive function of Krüppel homolog 1 on insect metamorphosis in hemimetabolous and holometabolous species. *Sci. Rep.* **1**, 163 (2011).
34. Lozano, J. & Belles, X. Role of methoprene-tolerant (Met) in adult morphogenesis and in adult ecdysis of *Blattella germanica*. *PLoS ONE* **9**, e103614 (2014).
35. Tian, L. et al. 20-hydroxyecdysone upregulates *Atg* genes to induce autophagy in the Bombyx fat body. *Autophagy* **9**, 1172–1187 (2013).
36. Jia, Q. et al. Juvenile hormone and 20-hydroxyecdysone coordinately control the developmental timing of matrix metalloproteinase-induced fat body cell dissociation. *J. Biol. Chem.* **292**, 21504–21516 (2017).
37. Eliyahu, D., Nojima, S., Mori, K. & Schal, C. Jail baits: how and why nymphs mimic adult females of the German cockroach, *Blattella germanica*. *Anim. Behav.* **78**, 1097–1105 (2009).
38. Schal, C., Burns, E. L., Jurenka, R. A. & Blomquist, G. J. A new component of the female sex pheromone of *Blattella germanica* (L.) (Dictyoptera: Blattellidae) and interaction with other pheromone components. *J. Chem. Ecol.* **16**, 1997–2008 (1990).

Acknowledgements

We thank D. Nelson for naming of *CYP4PC1*, D. Huang for preparing the cockroach cartoon and Z. Wang and X. Yi for assistance on Python and R software. We are grateful to W. Wang, Q. Feng, X. He, C.X. Zhang and S. Zhan for their comments and suggestions to improve the manuscript. This work was supported by the National Natural Science Foundation of China (grant nos. 31930014 to S.L., 32100378 to N.C. and 31772533 to Y.-L.F.), the Department of Science and Technology in Guangdong Province (grant nos. 2019B090905003 and 2019A0102006 to S.L.), the Laboratory of Lingnan Modern Agriculture Project (grant no. NT2021003 to S.L.), the Shenzhen Science and Technology Program (grant no. KQTD20180411143628272 to S.L.) and the China Postdoctoral Science Foundation (grant no. 2019M652941 to N.C.).

Author contributions

Conceptualization was done by S.L., N.C., Y.-L.F. and C.S. The methodology was developed by N.C., Y.-J.L., M.-T.L. and N.L. The investigation was carried out by N.C., Y.-J.L., X.-J.P., Y.Y. and J.Z. Visualization was done by N.C. and Y.-J.L. Funding was acquired by S.L., Y.-L.F. and N.C. Project administration was the responsibility of N.L. Supervision was done by S.L., Y.-L.F., G.W., Y.P. and C.S. The original draft was written by N.C. and Y.-L.F. Review and editing of the draft was done by S.L., C.S., Y.P., G.W. and T.-X.L.

Competing interests

The authors declare no competing interests.

Additional information

Extended data are available for this paper at https://doi.org/10.1038/s41559-022-01808-w.

Supplementary information The online version contains supplementary material available at https://doi.org/10.1038/s41559-022-01808-w.

Correspondence and requests for materials should be addressed to Yong-Liang Fan or Sheng Li.

Peer review information *Nature Ecology & Evolution* thanks Xavier Belles and the other, anonymous, reviewer(s) for their contribution to the peer review of this work. Peer reviewer reports are available.

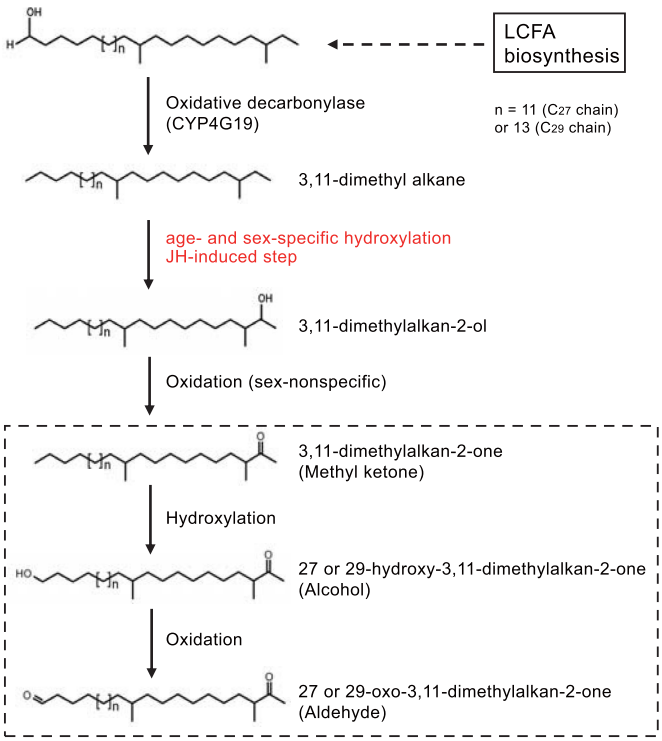

Extended Data Fig. 1 | Schematic diagram of the CSP biosynthetic pathway in *Blattella germanica*. A blend of six structurally related CSP components (in black dashed box) share a common biosynthetic pathway, in which the methyl ketones are formed by age- and sex-specific hydroxylation (in red text, the rate-limiting step possibly mediated by a cytochrome P450 system) of the 3,11-dimethyl alkane precursors and subsequent oxidation[13]. LCFA, long-chain fatty acid.

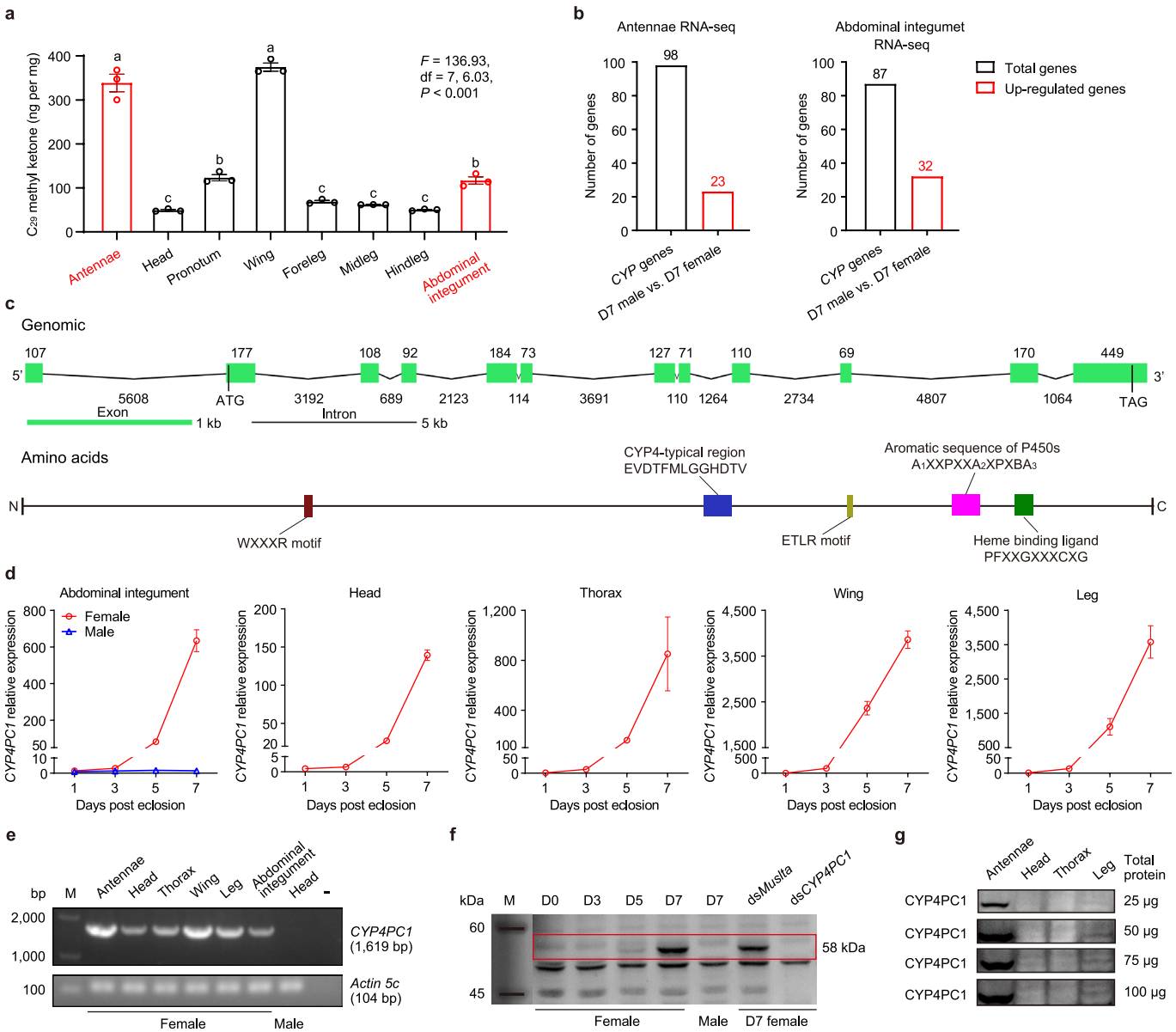

Extended Data Fig. 2 | Screening of the female-specific *CYP4PC1* by RNA-seq and its expression profiling. a, Distribution of cuticular C_{29} methyl ketone titre in sexually mature females. The antennae and abdominal integument (in red text and bar) were used for RNA-seq analyses. $n = 3$ biological replicates. Different letters indicate statistically significant differences between groups using Welch's ANOVA (Games-Howell multiple comparisons test, $P < 0.05$). Data are mean ± s.e.m. **b**, The numbers of total *CYP* genes identified in the antennae and abdominal integument, and those upregulated in sexually mature females compared to males. The FPKM values of the up-regulated *CYPs* are available in Supplementary Table 1, 2. **c**, Genomic organization of *CYP4PC1* and characteristic P450 motifs identified from the deduced protein sequence. The numbers nearby indicate the length of each exon or intron (base pair, bp), and conserved motifs typical of P450 are marked with colour-filled boxes. **d**, Developmental patterns of *CYP4PC1* expression in various tissues across sexual maturation. $n = 4$ biological replicates. Data are mean ± s.e.m. **e**, Gel electrophoresis verification of a 1,619 bp fragment containing the complete coding sequence of *CYP4PC1*, as amplified from various tissues by RT-PCR. A 104 bp fragment of *actin-5c* was used as a loading control. M, DNA marker. -, negative control with no DNA template. **f**, Western blotting validation of the CYP4PC1 antibody using antennal protein extracts and RNAi experiment. The red frame indicates immune signals of the endogenous CYP4PC1 protein, with a predicted molecular weight of 58 kDa. M, protein marker. The lane of protein markers was spliced from the white light image of the same membrane. **g**, Dose-dependent CYP4PC1 protein level in various tissues resulted from a gradient of total protein loaded, as determined by western blotting.

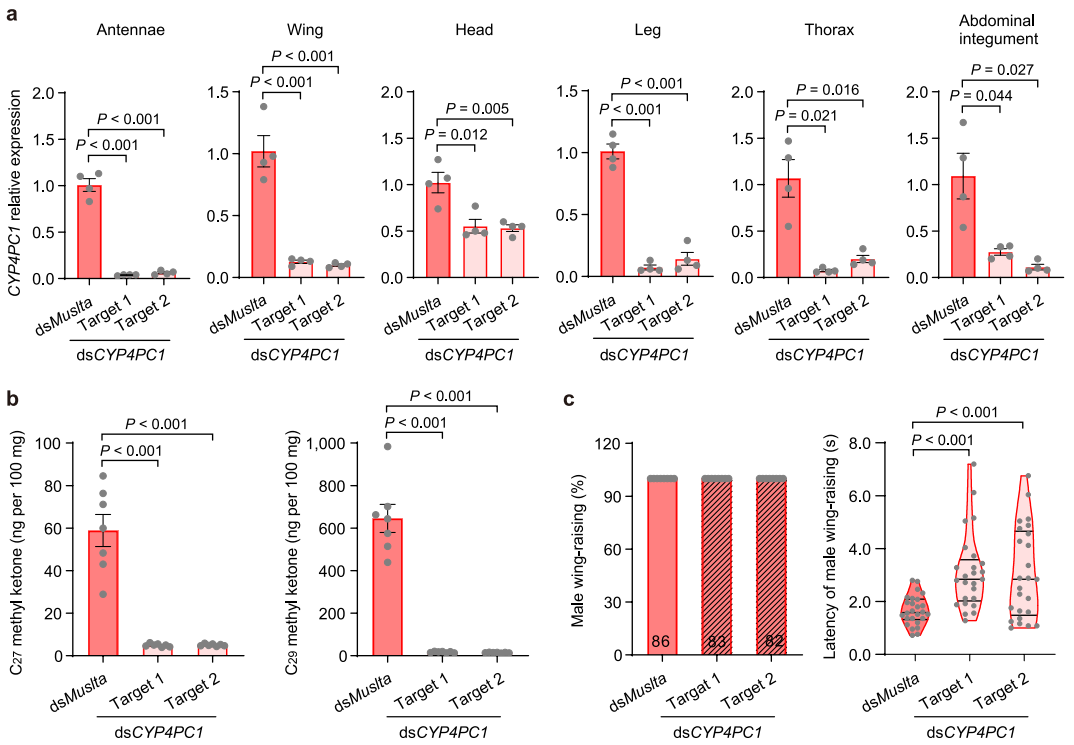

Extended Data Fig. 3 | *CYP4PC1* controls methyl ketone CSP production and female sexual attractiveness. a, RNAi efficiency in various tissues of adult females after two injections of dsRNA, each on day 1 and day 3, as determined by qPCR on day 5. $n = 4$ biological replicates. **b**, C_{27} and C_{29} methyl ketone CSP production resulted from *CYP4PC1* knockdown in adult females. $n = 7$ biological replicates. **c**, Effect of *CYP4PC1* knockdown in adult females on the wing-raising percentage and the latency of wing-raising in WT males. The numbers of tested males from eight behavioural replicates are indicated at the bottom of the bars. $n = 26$ cockroaches per treatment for the right panel. The solid line and dashed lines within each violin plot indicate median and quartiles, respectively. *P* values were determined by two-tailed unpaired *t*-test. Data in all bar plots are mean ± s.e.m.

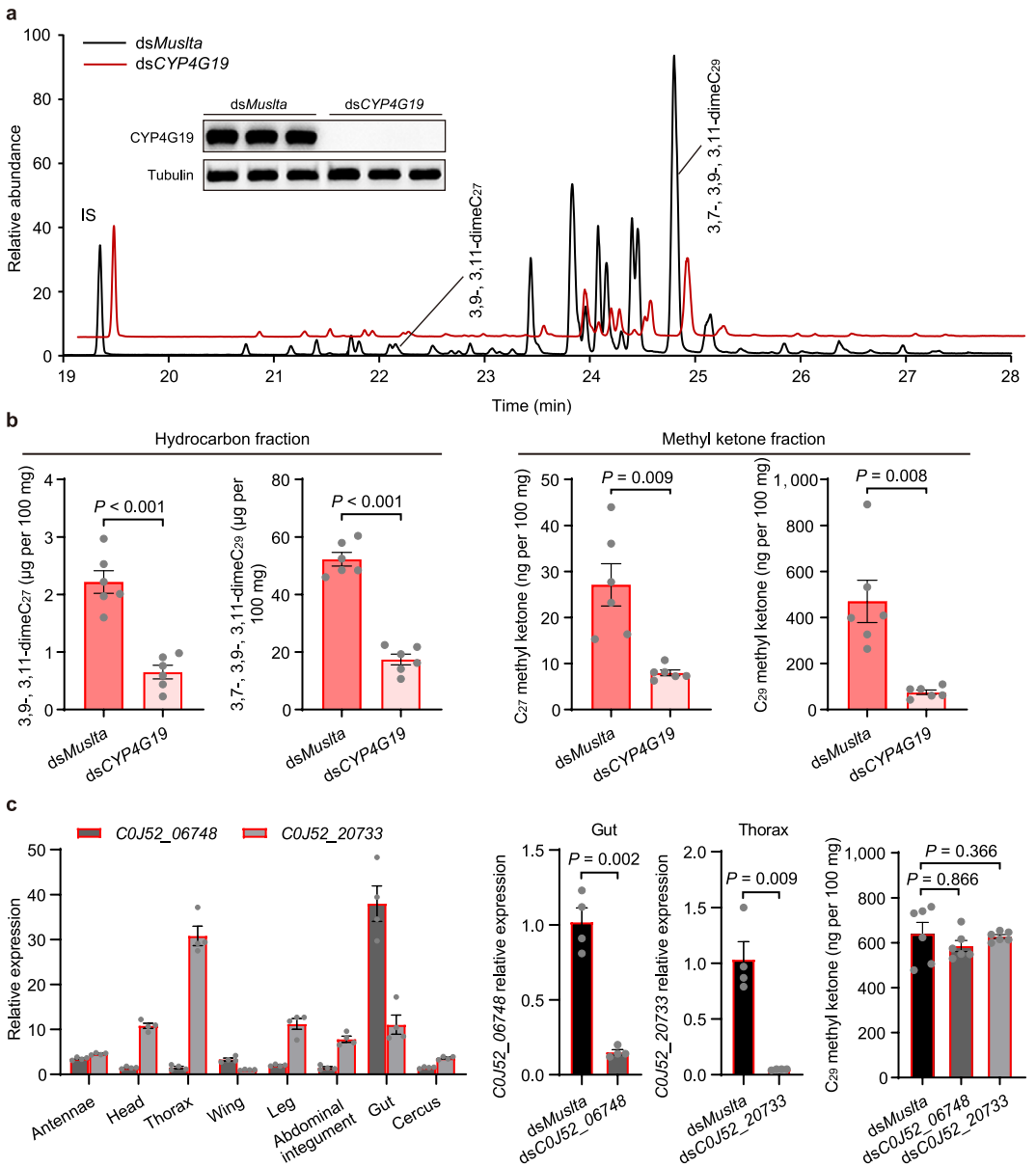

Extended Data Fig. 4 | *CYP4G19* modulates CSP production by affecting the biosynthesis of hydrocarbon precursors. a, RNAi knockdown of *CYP4G19* from N6 causes a depletion at the protein level (inset) and downregulation in cuticular hydrocarbons in adult females. The bands of tubulin were spliced from those of ds*Muslta*- and ds*CYP4G19*-injected groups, each with three lanes, on the same membrane. IS, internal standard of *n*-hexacosane. Similar results were obtained from six biological replicates. **b**, Effects of *CYP4G19* knockdown on dimethyl alkane and methyl ketone production. $n = 6$ biological replicates. **c**, Tissue distribution of two other *CYP* gene expressions in adult females and the effect of their knockdown on CSP production. $n = 4$ (gene relative expression) and 6 (methyl ketone production) biological replicates. *P* values were determined by two-tailed unpaired *t*-test (**b**, **c**). Data in bar plots are mean ± s.e.m.

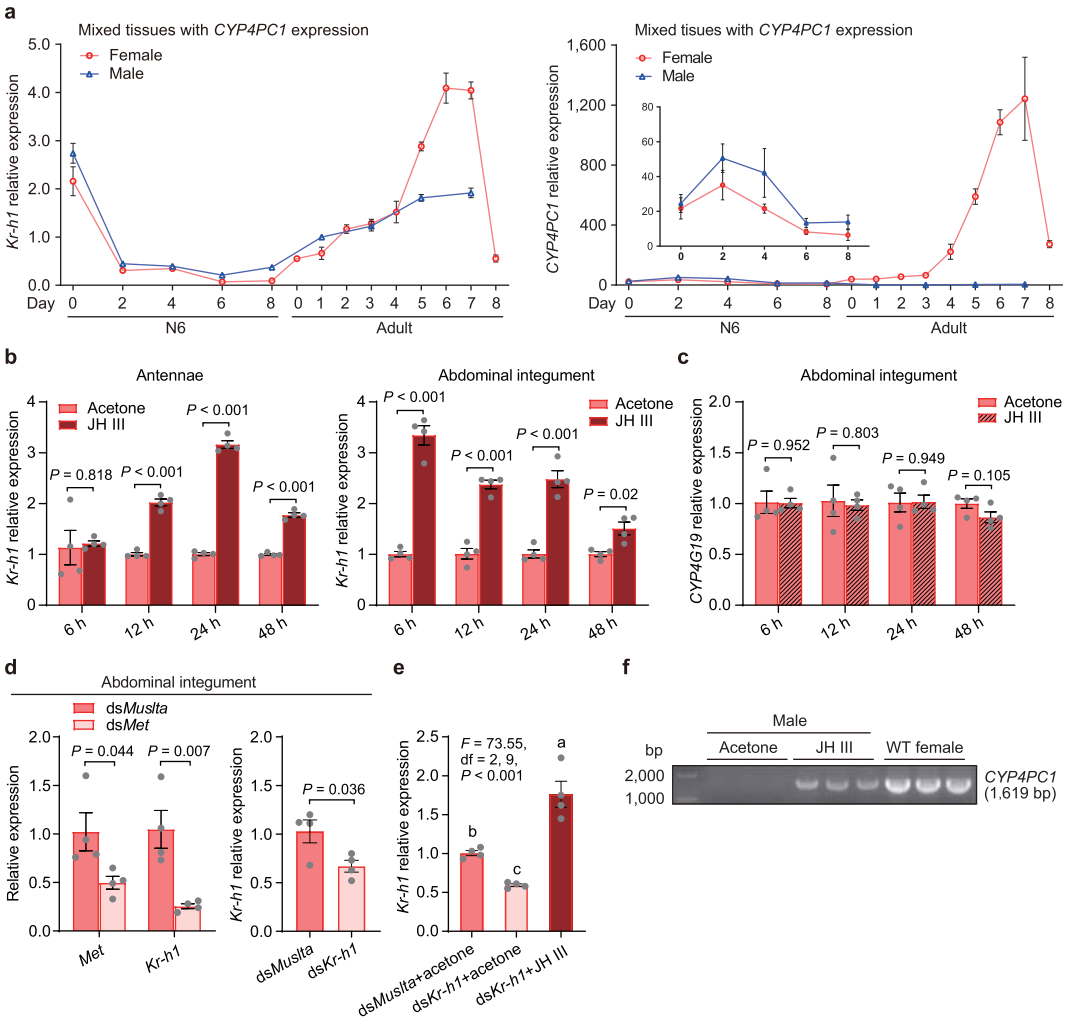

Extended Data Fig. 5 | JH signalling regulates the expression of *CYP4PC1* but not *CYP4G19*. **a**, Developmental similarity of *Kr-h1* and *CYP4PC1* expression across N6 and the first vitellogenic cycle. Inset of the right panel indicates a magnification of *CYP4PC1* expression throughout N6. $n = 4$ biological replicates. **b**, **c**, Effect of JH III treatment in adult females on *Kr-h1* expression in the antennae and abdominal integument (**b**), and *CYP4G19* expression in the abdominal integument (**c**). $n = 4$ biological replicates. **d**, RNAi knockdown of *Met* or *Kr-h1* in adult females is efficient in the abdominal integument. $n = 4$ biological replicates. **e**, *Kr-h1* relative expression in the antennae from females with *Kr-h1* knockdown and those with both ds*Kr-h1* and JH III treatments. $n = 4$ biological replicates. **f**, JH III application in adult males causes substantial transcription of *CYP4PC1* in the antennae. The complete coding sequence of *CYP4PC1* was detected in the antennae. *P* were determined by two-tailed unpaired *t*-test (**b**–**d**). Different letters indicate significant differences using one-way ANOVA (Tukey HSD multiple comparisons test, $P < 0.05$) (**e**). Data in **a**–**e** are mean ± s.e.m.

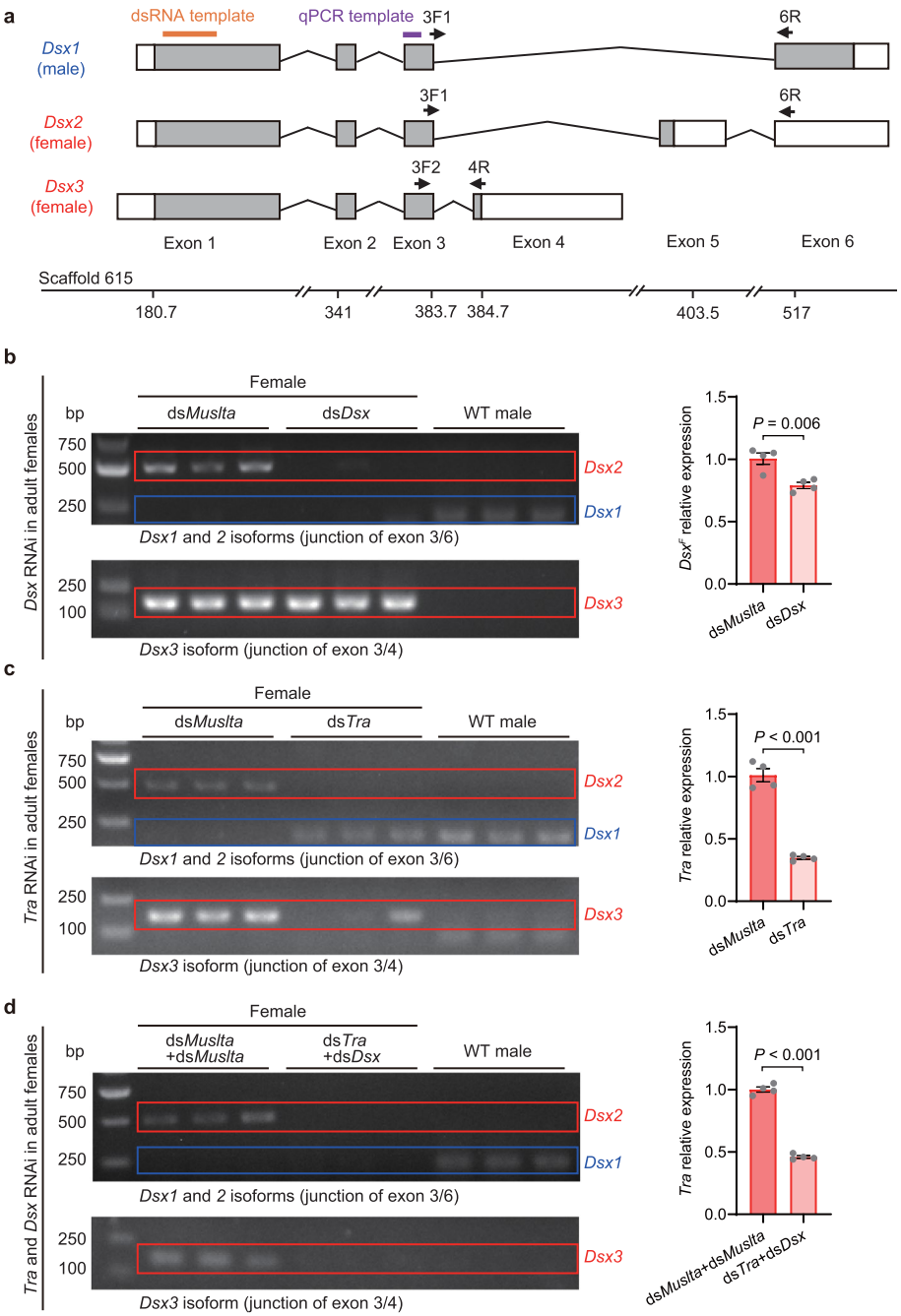

Extended Data Fig. 6 | The *tra-dsx* sex differentiation pathway promotes *CYP4PC1* expression in females. a, A diagram showing *dsx* splicing isoforms in *B. germanica* males and females. The modified diagram is based on a previous study[28]. All the primers used for dsRNA synthesis, qPCR analysis, and RT-PCR are summarized in Supplementary Table 3. **b**, Knockdown of dsx^F (*dsx2* and *3*) results in a depletion of *dsx2* but not *dsx3*. **c**, Knockdown of *tra* in adult females affects the alternative splicing between dsx^F and dsx^M. **d**, Effect of double knockdown of both *tra* and *dsx* in adult females on *dsx* isoforms. *P* values were determined by two-tailed unpaired *t*-test (**b**–**d**). Data in bar plots are mean ± s.e.m from four biological replicates.

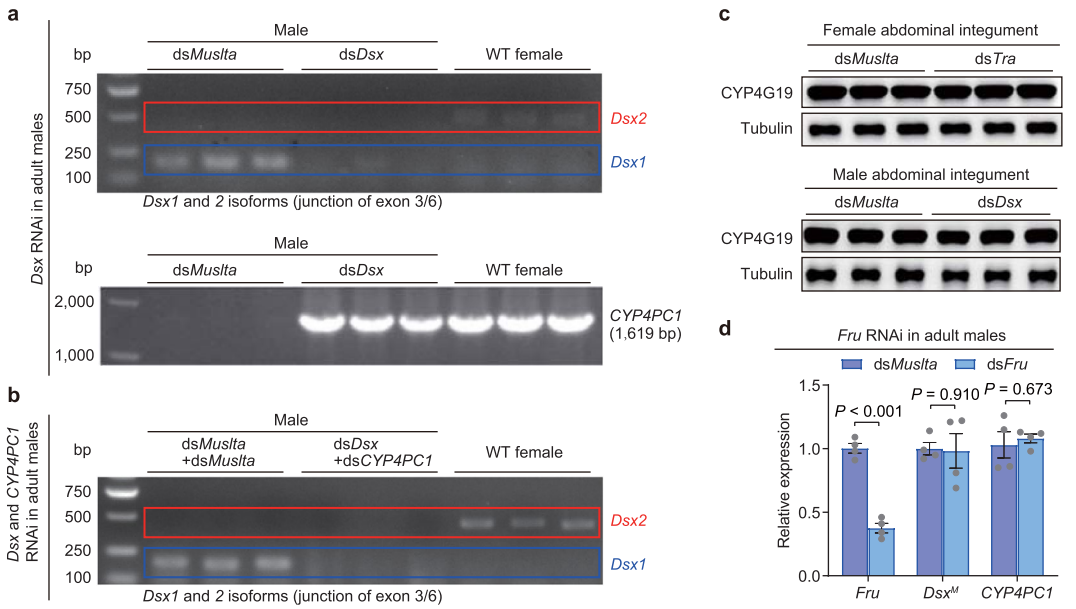

Extended Data Fig. 7 | Dsx^M represses *CYP4PC1* expression in males. a, Knockdown of *dsx* in adult males promotes *CYP4PC1* transcript. The complete coding sequence of *CYP4PC1* was detected in the antennae of ds*Dsx*-treated adult males. **b**, Effect of double knockdown of both dsx^M and *CYP4PC1* in adult males on *dsx* isoforms. **c**, Knockdown of *tra* in adult females or *dsx* in adult males has no effect on CYP4G19 protein level. **d**, Effect of *fru* knockdown in adult males on dsx^M and *CYP4PC1* expressions. $n = 4$ biological replicates. *P* values were determined by two-tailed unpaired *t*-test. Data are mean ± s.e.m.

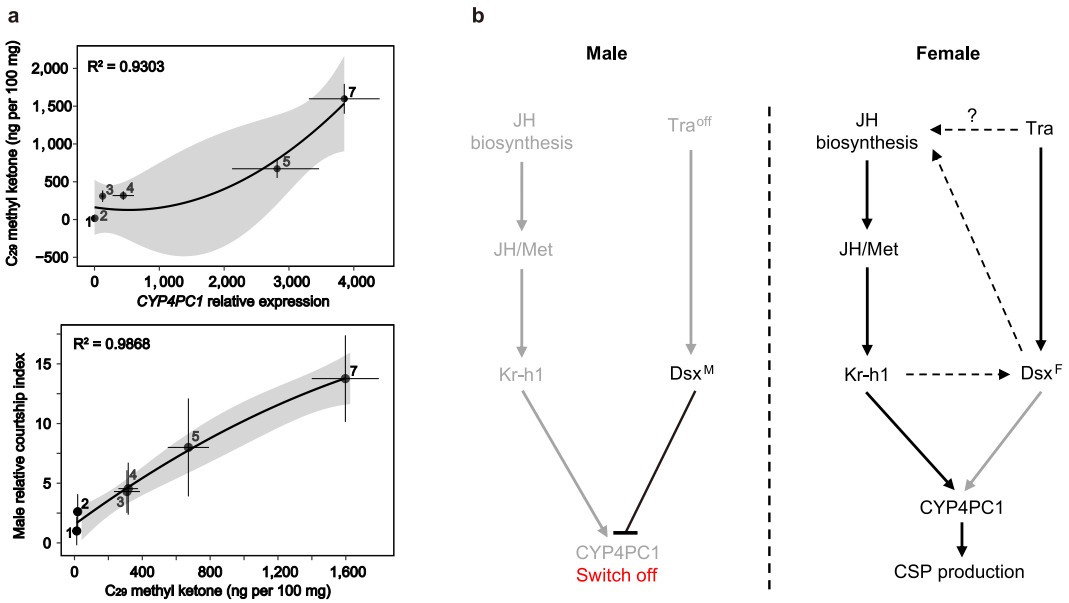

Extended Data Fig. 8 | *CYP4PC1* integrates sex differentiation and hormone signalling pathways and controls sexual attractiveness in a dose-dependent manner. a, Curve fitting between *CYP4PC1* expression and CSP production, and CSP production and male courtship index. The 95%CI is shown in grey. The source data are derived from groups 1–5 and 7 in Fig. 6a. Data are mean ± s.d. **b**, A schematic summary showing the regulatory network of *CYP4PC1* expression. Such a mechanism ensures female-specific *CYP4PC1* expression (*dsx*-dependent) and high level CSP production upon sexual maturation (JH-dependent).

nature portfolio

Corresponding author(s): Sheng Li

Last updated by author(s): May 14, 2022

Reporting Summary

Nature Portfolio wishes to improve the reproducibility of the work that we publish. This form provides structure for consistency and transparency in reporting. For further information on Nature Portfolio policies, see our Editorial Policies and the Editorial Policy Checklist.

Statistics

For all statistical analyses, confirm that the following items are present in the figure legend, table legend, main text, or Methods section.

n/a	Confirmed	
☐	☒	The exact sample size (*n*) for each experimental group/condition, given as a discrete number and unit of measurement
☐	☒	A statement on whether measurements were taken from distinct samples or whether the same sample was measured repeatedly
☐	☒	The statistical test(s) used AND whether they are one- or two-sided *Only common tests should be described solely by name; describe more complex techniques in the Methods section.*
☐	☒	A description of all covariates tested
☐	☒	A description of any assumptions or corrections, such as tests of normality and adjustment for multiple comparisons
☐	☒	A full description of the statistical parameters including central tendency (e.g. means) or other basic estimates (e.g. regression coefficient) AND variation (e.g. standard deviation) or associated estimates of uncertainty (e.g. confidence intervals)
☐	☒	For null hypothesis testing, the test statistic (e.g. *F*, *t*, *r*) with confidence intervals, effect sizes, degrees of freedom and *P* value noted *Give P values as exact values whenever suitable.*
☒	☐	For Bayesian analysis, information on the choice of priors and Markov chain Monte Carlo settings
☒	☐	For hierarchical and complex designs, identification of the appropriate level for tests and full reporting of outcomes
☒	☐	Estimates of effect sizes (e.g. Cohen's *d*, Pearson's *r*), indicating how they were calculated

Our web collection on statistics for biologists contains articles on many of the points above.

Software and code

Policy information about availability of computer code

Data collection	Illumina HiSeq2000, Illumina Novaseq6000, Xcalibur 2.2 (Thermo Scientific), video recording system (Hikvision, Hangzhou, China)
Data analysis	Hisat2, Trinity program, Xcalibur 2.2 (Thermo Scientific), SPSS 19.0, R software, Python 3.7, Graphpad Prism 8.0.2, and Illustrator CC

For manuscripts utilizing custom algorithms or software that are central to the research but not yet described in published literature, software must be made available to editors and reviewers. We strongly encourage code deposition in a community repository (e.g. GitHub). See the Nature Portfolio guidelines for submitting code & software for further information.

Data

Policy information about availability of data

All manuscripts must include a data availability statement. This statement should provide the following information, where applicable:

- Accession codes, unique identifiers, or web links for publicly available datasets
- A description of any restrictions on data availability
- For clinical datasets or third party data, please ensure that the statement adheres to our policy

Sequence data of CYP4PC1 gene has been deposited in GenBank with the accession code MZ962381. All data and materials to understand and assess the conclusions of this research are available within the Article, Extended Data, Source Data, and the Supplementary files, and via the Sequence Read Archive (SRA) database under accession numbers PRJNA759392 and PRJNA760811.

Field-specific reporting

Please select the one below that is the best fit for your research. If you are not sure, read the appropriate sections before making your selection.

☒ Life sciences ☐ Behavioural & social sciences ☐ Ecological, evolutionary & environmental sciences

For a reference copy of the document with all sections, see nature.com/documents/nr-reporting-summary-flat.pdf

Life sciences study design

All studies must disclose on these points even when the disclosure is negative.

Sample size	Sample size for qPCR, western blot, luciferase reporter assay, chemical analysis, behavioral assays was determined on the basis of previous studies in our laboratory (Chen et al., 2020; Pei et al., 2021; Zhu et al., 2020; Jia et al., 2017).
Data exclusions	No data were excluded from the analyses.
Replication	All quantifications were done on a minimum of three independent biological replicates.
Randomization	The samples were allocated randomly into experimental groups.
Blinding	For behavioral experiments, the investigators were blinded to group allocation during data collection and data analysis. For the other experiments, the investigators were not blinded during data collection and analysis, as most of the experiments were randomly performed by two major researchers.

Reporting for specific materials, systems and methods

We require information from authors about some types of materials, experimental systems and methods used in many studies. Here, indicate whether each material, system or method listed is relevant to your study. If you are not sure if a list item applies to your research, read the appropriate section before selecting a response.

Materials & experimental systems

n/a	Involved in the study
☐	☒ Antibodies
☐	☒ Eukaryotic cell lines
☒	☐ Palaeontology and archaeology
☐	☒ Animals and other organisms
☒	☐ Human research participants
☒	☐ Clinical data
☒	☐ Dual use research of concern

Methods

n/a	Involved in the study
☒	☐ ChIP-seq
☒	☐ Flow cytometry
☒	☐ MRI-based neuroimaging

Antibodies

Antibodies used	Affinity-purified polyclonal antibody against CYP4PC1 or CYP4G19 (rabbit) was developed in Wuhan GeneGreate Biological Engineering Company, China. (1:5000) Mouse monoclonal anti-Tubulin antibody (1:5000) (Beyotime, China) Anti-rabbit or -mouse IgG secondary antibodies (both 1:5000) (Beyotime, China) Rabbit monoclonal His-Tag antibody (1 µL per EMSA reaction) (Cell Signalling Technologies)
Validation	The CYP4PC1 and CYP4G19 antibodies were validated by Elisa and Western blot. The antibody against Tubulin and anti-rabbit or -mouse IgG secondary antibody are commercially available, and were validated by the manufacturer and our previous study (Zhu et al., 2020). Rabbit monoclonal His-Tag antibody was validated by the manufacturer.

Eukaryotic cell lines

Policy information about cell lines

Cell line source(s)	Drosophila Kc cell line was originally purchased from Thermo Fisher Scientific and was maintained in our laboratory.
Authentication	The used cell line in this study is commercially available, and was authenticated by the manufacturer.
Mycoplasma contamination	All cells were tested for mycoplasma and proven negative.

Commonly misidentified lines (See ICLAC register)	No commonly misidentified cell lines were used.

Animals and other organisms

Policy information about studies involving animals; ARRIVE guidelines recommended for reporting animal research

Laboratory animals	The cockroaches (Blattella germanica, females and males, nymphs and adults) used in the experiments were maintained in the Institute of Insect Science and Technology, South China Normal University, Guangzhou, China.
Wild animals	The study did not involve wild animals.
Field-collected samples	The study did not involve samples collected from the field for laboratory work.
Ethics oversight	No ethical approval or guidance was required for the experiments using cockroach samples.

Note that full information on the approval of the study protocol must also be provided in the manuscript.